

國立臺灣大學生命科學院動物學研究所

碩士論文

Institute of Zoology

College of Life Science

National Taiwan University

Master Thesis

大鼠未定核對視丘後內側核傳遞

傷害性傳入訊息之調控

**Zona Incerta modulation of posterior medial nucleus
processing of nociceptive information in the rat**

王 楹

Ying Wang

指導教授：嚴震東 博士

Advisor: Chen-Tung Yen, Ph.D.

中華民國 98 年 7 月

July, 2009

國立臺灣大學碩士學位論文
口試委員會審定書

大鼠未定核對視丘後內側核傳遞
傷害性傳入訊息之調控

Zona Incerta modulation of posterior medial nucleus
processing of nociceptive information in the rat

本論文係王楹君 (R94B41006) 在國立臺灣大學生命科學系動物學研究所完成之碩士學位論文，於民國九十八年七月十三日承下列考試委員審查通過及口試及格，特此證明

口試委員：

嚴震東

(簽名)

(指導教授)

黃其斌

劉研源

齊任琦

系主任、所長

陳俊彥

(簽名)

誌謝

回想兩年前的我，剛進入這個實驗室，最喜歡拿學長姐的論文來"參考參考"，為的不是別的，就是想看致謝。大概是想從那些甚至從未謀面的學長姐中，偷得一點點畢業的感動吧！兩年過去了，今天終於輪到我分享這份感動。

首先，我要感謝我的指導老師—嚴震東老師，一點也不嫌棄的接納我這個從工作中返回學校的學生。在我研究所生涯的兩年裡，老師教給我的不僅僅是神經腦科學的知識，從平常的談話與相處中，更令我深深的感受到老師耿直的為人與做研究的熱誠，很榮幸也很感謝老師讓我有機會能成為老師的學生。感謝實驗室裡的另一個老師—陳瑞芬老師，陳老師總是像媽媽一樣的鼓勵我們、給我們溫暖與照顧，在我實驗不順利的時候與開朗的陳老師聊上幾句，總能讓我重新振作精神再出發。另外，也很感謝實驗室今年的客座老師—胡偉老師，胡老師不但在課堂上給我們良好扎實的訓練，也會主動關心我們的實驗近況，樂於給我們建議與協助，感謝老師無私的幫忙，使我的實驗終於能從「清水變雞湯」了！最後我要特別感謝以前在師大的指導老師—黃基礎老師，大學時代的我總是害怕手術失敗而不願多做幾次實驗，但老師卻從不曾對這樣的我有所微詞，如果不是黃老師當初的諒解與包容，我想我不會毅然決然的在工作兩年後還決定要回學校念研究所，也不會選擇當初害怕的電生理領域，更不會有今天的口試畢業，真的很感謝黃老師，謝謝老師教會了我作為一個老師，有時候該給予的不是逼迫，而是接納。

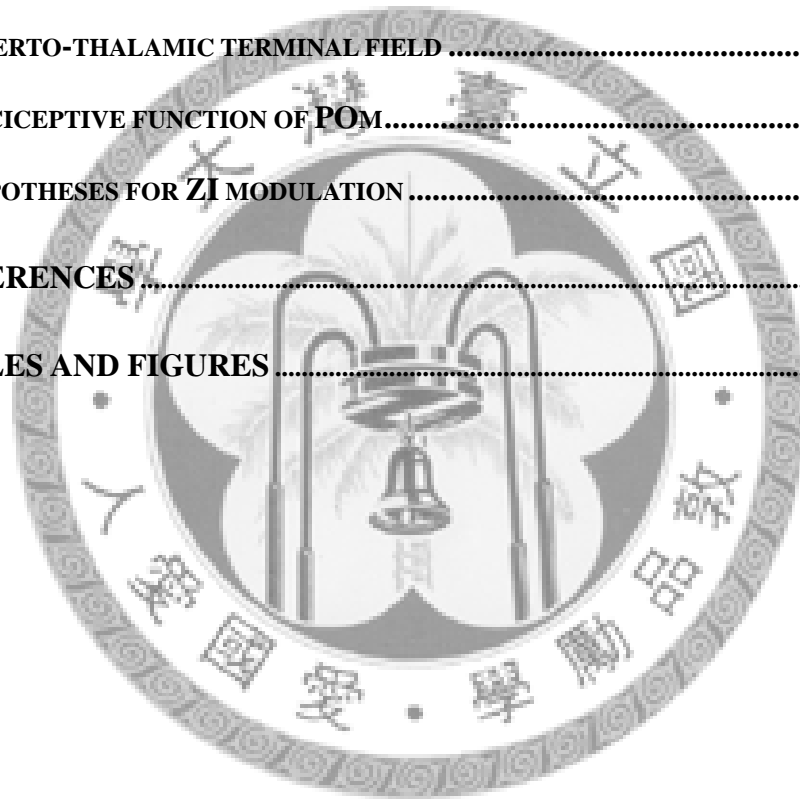
除了老師們，在這兩年裡認識的實驗室的好伙伴們，更是支持我能夠繼續做實驗的動力！感謝同時是學姊也是我的口委的佳琦學姊，總是給我正面的鼓勵與支持，親切的和我分享生活上的點點滴滴，和你相處永遠不會有壓力；感謝儀芳學姊，除了讓我在搜尋ZI的路上沒吃過苦頭外，在我實驗不順、心情沮喪的時候和你深談總能「化解」我心裡的黑雲；感謝實驗神手婉婷學姊，不厭其煩的幫我修改程式，陪著我做令我害怕的實驗，沒有你實驗操作上的小撇步與完美的程式，我真的很難完成這本論文；另外，實驗室的下一任開心果—庭芳學妹，謝謝你常在我緊張的時候安慰我，還幫我按摩！你大方又可愛的個性真是讓人喜歡！實驗室的助理妍微，我永遠不會忘記剛進實驗室你親切又溫柔的招呼我，你有著我最喜歡的特質—善良，以後還要一起聊養狗經！互相交換恐怖片！還有大方海派很會照顧人的學姊瑞珍，外表冷酷但內心似乎是小男孩的可愛學長白峯，陪著我一起去日本研討會、對我照顧有加的學姊本立，積極正面且總是抱持樂觀想法的好同學慧馨，知識淵博總是不吝於指導學弟妹的校群學長，實驗高手建嘉學長，以及剛進來實驗室的學弟妹智羽、郁昕、旭偉…。還有一定要感謝的是永遠給我無私的愛與關懷的爸爸、媽媽、拉奇寶，還有總是當我情緒抒發的垃圾桶的Water兄。真的很感謝大家這兩年的陪伴與支持，使我在研究所的這一路上都不曾孤單！

我永遠不會忘記大家的，請大家也不要忘記我喔！：)

Table of Contents

1. 中文摘要	3
2. ABSTRACT	4
3. INTRODUCTION	5
3.1. FUNCTIONAL ROLES OF THE POM.....	6
3.2. INHIBITION CONTROL FROM THE ZI	7
3.3. GOAL OF THE STUDY	8
4. MATERIALS AND METHODS.....	10
4.1. EXPERIMENT 1. ANTEROGRADE TRACING STUDY.....	10
4.1.1. Surgery preparation	10
4.1.2. Injections of bi-directional tracer	10
4.1.3. Fixation and immunohistochemistry.....	11
4.1.4. Data analysis.....	12
4.2. EXPERIMENT 2. ELECTROPHYSIOLOGICAL EXPERIMENTS.....	12
4.2.1. Kainic acid lesion	12
4.2.2. Surgery preparation	13
4.2.3. Extracellular single-unit recording	13
4.2.4. Data acquisition and analysis.....	15
4.2.5. Histology	17
4.2.6. Immunohistochemistry for parvalbumin	17
5. RESULT.....	19
5.1. I ANTEROGRADE TRACING STUDY.....	19
5.1.1. Electrophysiological identification of ZI.....	19

5.1.2. B. BDA injection in the ZI.....	20
5.2. II. ELECTROPHYSIOLOGICAL EXPERIMENTS	21
5.2.1. Lesion of ZI.....	22
5.2.2. Response of POm and VP neurons to mechanical stimulation	22
5.2.3. Response of POm and VP neurons to contact thermal stimulation	25
5.2.4. Cell locations.....	26
6. DISCUSSION	27
6.1. INCERTO-THALAMIC TERMINAL FIELD	27
6.2. NOCICEPTIVE FUNCTION OF POM.....	28
6.3. HYPOTHESES FOR ZI MODULATION	31
7. REFERENCES	33
8. TABLES AND FIGURES	36



摘要

前人研究顯示大鼠視丘後內側核(POm)會受到未定核(ZI)持續且有力的抑制性調控，因此 ZI 移除後，才能見到 POm 神經元對輕觸鬚鬚之刺激產生明顯的反應。本研究目的是檢視 ZI 被毀壞後，POm 調控傷害性傳入訊息的能力。首先利用神經追蹤劑檢視 ZI 投射至 POm 的確切區域。而後在 ZI 經過毀壞的實驗動物上，以 16 通道—密西根電極進行單一神經元紀錄。本實驗在 ZI 毀壞同側之 POm 紀錄到了 42 顆神經元，在 ZI 毀壞側之對側與未經手術的動物紀錄了 81 顆神經元，比較這些神經元對於傷害性機械刺激與熱痛刺激的反應。研究結果顯示：1) ZI 被毀壞後，POm 中對傷害性刺激有反應的神經元數目顯著高於對照組；2) 藉由 ZI 的調控，POm 可能為一傳遞傷害性刺激訊息的區域。本實驗藉由 ZI 移除的處理，揭開了隱藏於 POm 傳遞傷害性訊息之能力。然此能力在正常動物中的重要性仍需進一步的研究與探討。



Abstract

The posterior medial nucleus (POM) is tonically inhibited by Zona Incerta (ZI), so that robust vibrissae evoked responses are revealed after ZI inactivation. The present study was to examine the capability of the POM neurons in processing nociceptive information after removal of ZI inhibition. Incerto-POM terminal zones were delineated by anterograde tracing of Biotinylated Dextran Amine. For electrophysiological studies, unilateral ZI lesion was made by micro-injection of kainic acid into the facial region of ZI. Seven days after lesion, single-unit recordings were made with a 16-channel Michigan probe. Responses to noxious mechanical and thermal stimuli were compared among 42 POM neurons in ZI lesioned sides versus 81 neurons in non-lesioned side and naïve animals. Our results showed that, 1) the percentage of nociceptive neurons in POM of the ZI lesioned rats were significantly higher than those of the controls; 2) POM may be a conditional nociceptive processing region depending on ZI modulation. Our data unveiled the hidden nociceptive processing capability of the POM in ZI removed condition. How this capability is used in normal animals awaits further studies.

Introduction

The thalamus is the gateway for the processing of somatosensory information. Within the thalamus, there are three important parts namely, the ventroposterior, medial thalamic nuclei and posterior complex. In rodents, there are two major trigemino-thalamic nuclei that relayed vibrissa-related information to the somatosensory cortex: 1) the lemniscal ventroposterior medial (VPM) nucleus that receives vibrissae inputs primarily from the principal trigeminal nucleus (PrV), and 2) the paralemniscal posterior medial nucleus (POm) whose vibrissae responses originate both from ascending inputs from the trigeminal nucleus interpolaris (SpVi) and from descending inputs from the barrel cortex (Yu et al., 2006). Because of the importance of the somatosensory transmission in rodent whiskers system, there are many studies focus on the paralemniscal pathway in the anatomical ground (Chiaia et al., 1991; Iwata et al., 1992; Alloway et al., 2003; Gauriau and Bernard, 2004a), however, fewer studies have been done on the functional role of POm, especially in the pain function.

POm is one of the nuclei in the posterior complex. It lies dorsal to the VP and extends back along the medial edge of the medial geniculate complex. In rats, the anterior part of the POm, dorsal to the VP, is quite different from the posterior part in connectional and physiological aspects (Diamond et al., 1992a; Gauriau and Bernard,

2004b). The posterior part of POM in rodents, where it lies along the medial edge of the medial geniculate complex, has been studied by many investigators due to the high sensitivity to noxious stimulation. It is separated from POM and delineated as triangular posterior nucleus (PoT) (Gauriau and Bernard, 2004a). The present study is concentrated on the anterior part of POM, which will be named as “POM” following the accepted literature (Diamond et al., 1992a; Diamond et al., 1992b).

Functional roles of the POM

In anesthetized rats, responses of VP neurons to whiskers deflections are robust and of short latency, while responses of POM neurons are weak and their latency longer (Diamond et al., 1992b). Unlike VP cells, which remain sensitive to whiskers deflections when the barrel cortex is inactivated, POM cells, despite a peripheral connection from the trigeminal complex and spinal cord, their activities seem to depend on an intact barrel cortex (Diamond et al., 1992a). Because of the unreliable responses of POM, the functional role of POM and paralemniscal pathway is more obscure and difficult to study.

Some researchers indicate that the POM neurons can code the stimulus frequency as changes in onset latency. They discovered that as the onset latencies increased and the offset latencies remained constant, which means that the latency increments were translated into a rate code: increasing onset latencies led to lower spikes counts.

Therefore, they hypothesized that the POM is involved in temporal processing related to sensory-motor control of whisker movement (Ahissar et al., 2000; Yu et al., 2006). However, another group of researchers tested the hypothesis in awake, head-restrained rats and suggested that POM neurons might not be involved in temporal processing. In stead, they propose that POM may be preferentially involved in processing of nociceptive inputs on anatomical grounds (Masri et al., 2008). Indeed, several anatomical reports indicate that the POM receives dense projections from superficial laminar of dorsal horn, which many high-threshold neurons located in (Burstein et al., 1990; Gauriau and Bernard, 2004a; Guy et al., 2005). The references described above show that the precise function of POM is still under debated.

Inhibition control from the ZI

Recently, several reports indicate that another nucleus in thalamus, Zona incerta (ZI), can give inhibitory control to the POM. Therefore, after electronically or chemically lesion of ZI, some POM neurons can respond to whiskers deflections as robust and short-latency VP responses (Bartho et al., 2002; Trageser and Keller, 2004; Lavallee et al., 2005).

Located ventral to the medial lemniscus, ZI is a small collection of cells derived embryologically from the ventral thalamus (Jones, 2007). It has been implicated in a wide range of functions, including nociceptive and somatosensory processing

(Nicolelis et al., 1992), feeding and drinking (Gonzalez-Lima et al., 1993), arousal and attention (Hermanson et al., 1995), etc.

The wide-ranging functions may be the consequences of heterogeneity organization of the ZI, which made up of a heterogeneous group of cells and divided into several distinct sectors. Based on the cytoarchitecture and chemoarchitecture aspects, ZI can be divided into four sectors: rostral, dorsal, ventral and caudal in rats (Kim et al., 1992; Nicolelis et al., 1995). Among them, 80% of the cells in the ventral sector (ZIV) is GABA-immunoreactive (Kolmac and Mitrofanis, 1999). Several reports suggest that this part of ZI is tonically inhibiting the POM, so that robust vibrissae evoked tactile responses of the POM are revealed only after ZI lesion (Power et al., 1999; Bartho et al., 2002; Trageser and Keller, 2004; Lavallee et al., 2005). However, few studies test the nociceptive responses of POM neurons after ZI lesion.

Goal of the study

On anatomical grounds, POM receives nociceptive inputs from the spinal cord and medullary dorsal horn. However, few electrophysiological data exist that show POM contributes to nociceptive information transmission. Therefore, the goal of the present study was to test whether POM may convey nociceptive information after ZI lesion.

To test the hypothesis, anterograde tracing study was performed first to outline

the ZI receiving area in the POm. A zone of convergence was found with the putative nociceptive input. POm units in and around this convergent zone was recorded and tested for their nociceptive responses with or without ZI lesion. VP units were also examined for comparison basis.



Materials and Methods

Model organisms

A total of 32 adult male Wistar rats (300~400 g) were used in accordance with guidelines in the Codes for Experimental Use of Animals of the Council of Agriculture of Taiwan, based on the Animal Protection Law of Taiwan. All experimental protocols were approved by the Institutional Animal Care and Use Committee of National Taiwan University.

Experiment 1. Anterograde Tracing Study

Surgery preparation

This study was carried out in 5 rats. Rats were anesthetized with pentobarbital (i.p., 50 mg/kg). Throughout the experiment, the depth of anesthesia was maintained by supplementary doses of anesthetics given at 1-hour intervals. The core temperature of the rat was maintained at 37.5 °C by a feedback-controlled heating pad. After the rat was mounted on a stereotaxic apparatus, a unilateral craniotomy was made to expose the cortical areas above the ZIv (P: 4 mm, L: 2.6 mm) by referring to the atlas of Paxinos and Watson (Paxinos & Watson, 2005). In the sections that follow, all stereotaxic coordinates are given relative to the bregma.

Injections of bi-directional tracer

A bidirectional tracer, biotinylated dextran amine (BDA: 2 % in distilled water,

MW 10,000), was used. Glass micropipettes (tip size: 20~25 μ m, #602500, A-M system, Carlborg, WA) were filled with BDA solution and aimed for the ZIv (2.6 mm lateral, 4 mm posterior). The whiskers (n= 4) or the forepaw (n=1) responsive region of the ZI was identified by standard electrophysiological multi-unit recording and tested with light tapping to ensure the precise location of the injections sites. Then, BDA was ejected with positive current pulses (5 s duty cycles) of 5 μ A for 15 minutes. The micropipette was maintained in the injection sites for 30 minutes before withdrawing in order to minimize the backflow of the tracer. After the injection, the skin was sutured, and the rat was returned to the animal facilities.

Fixation and immunohistochemistry

After a survival of 7-10 days, the rat was deeply anesthetized with an overdose of pentobarbital (i.p., 75 mg/kg) and perfused with physiological saline followed by 4% paraformaldehyde in 0.1 M phosphate buffer at pH 7.4. The brain was then stored in 20% sucrose phosphate buffer (0.1 M, pH 7.4). Several days later, 50 μ m thick frozen sections were made serially in the coronal plane on a freezing microtome. And then the brain sections were rinsed in phosphate-buffered saline (PBS) and reacted with avidin-labeled peroxidase (ABC kit, PK-6100, Vector laboratories, Burlingame, CA) for an hour, and a diaminobenzidine-30% H₂O₂ solution for 10 minutes. Sections were mounted on gelatin-coated glass slides, air-dried, and hydrated with 100%

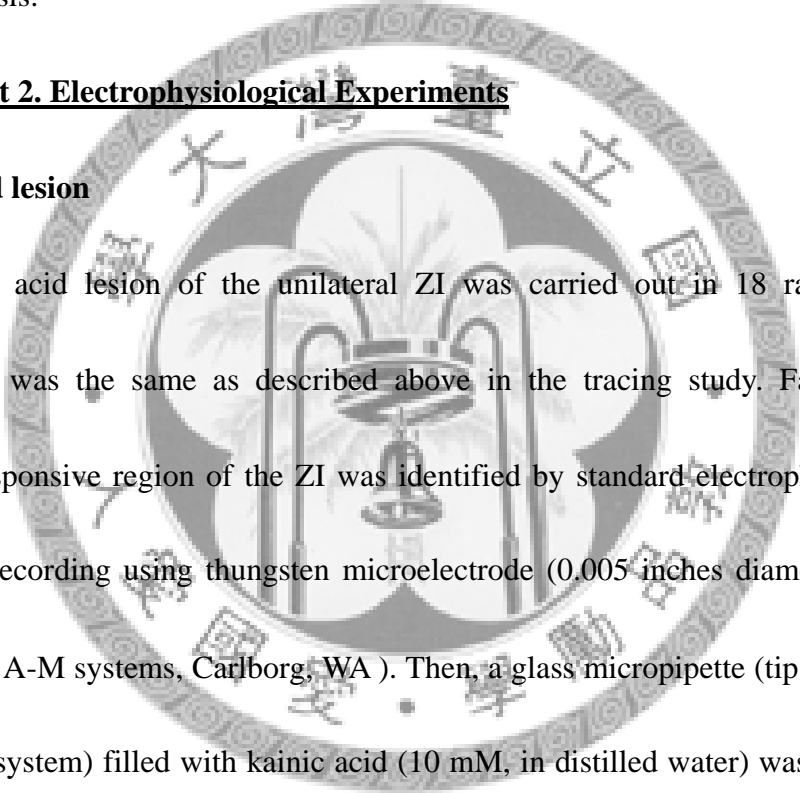
alcohol and coverslipped.

Data analysis

A microscope equipped with a digital camera was used to capture the images of the brain sections. Labeled fibers and boutons were photomicrographed and also documented with camera lucida drawings, and then scanned into Photoimpact 11 for detail analysis.

Experiment 2. Electrophysiological Experiments

Kainic acid lesion



Kainic acid lesion of the unilateral ZI was carried out in 18 rats. Surgery preparation was the same as described above in the tracing study. Facial or the forepaw responsive region of the ZI was identified by standard electrophysiological multi-unit recording using tungsten microelectrode (0.005 inches diameter, 5 M Ω impedance, A-M systems, Carlborg, WA). Then, a glass micropipette (tip size: 20~25 μ m, A-M system) filled with kainic acid (10 mM, in distilled water) was lowered in the same place, and the toxin was ejected 30~45 nL by pressure (pneumatic pump, PPS-2, Medical system corporation). The micropipette was maintained in the injection sites for 30 minutes before withdrawing to reduce the backflow of the toxin. The rat was allowed for 7~8 days recovery before electrophysiological experiment.

Surgery preparation

22 rats were used. Unilateral ZI lesion was made as described above in 13 of the rats. The rat was initially anesthetized by 3~5 % isoflurane and ketamine (i.m., 30 mg/kg). And then tracheal cannula was inserted. The anesthetic depth was maintained under 2 % isoflurane. A femoral vein was cannulated. Gallamine triethiodide (50 mg/kg) was administrated through the vein cannula at the interval of 60 minutes throughout the experimental period to immobilize the respiratory muscle. An adequate level of anesthesia was confirmed periodically by the lack of spontaneous movements and reflex responses when the gallamine-induced muscle paralysis was allowed to wear off. The whole face, including the whiskers, was shaved. Then the rat was mounted on a stereotaxic apparatus, and the dura mater over the foramen magnum was removed to relief the brain pressure to avoid brain tissue swelling and deformation. Craniotomies were made to expose the cortical areas above the thalamus (P: 2~5 mm, L: 1~4 mm) by referring to the atlas of Paxinos and Watson (Paxinos and Watson, 1998).

Extracellular single-unit recording

Single-unit activity was recorded extracellularly by Michigan probes (linear probe) (Fig. 1) held by a microdrive. Before all the penetrations, the probe was coded with HRP for confirming the penetration tract afterwards. As the probe penetrating

perpendicularly through the cortex into the brain tissue, natural mechanical stimuli were applied to the body surface to search for units responsive to the facial or forepaw stimulation.

Three experimental procedures were conducted. First, spontaneous activities of the neurons were recorded for 10 minutes. Second, mechanical stimulation was performed on the receptive field of the unit. The first stimulus in the mechanical stimulation was innocuous brushing with a soft-bristled brush, followed by a noxious pinching with a small artery clamp which can evoke pain sensation applied to the human subject. The duration of each stimulus was 15 s, and the stimulation interval is 30 s. Five minutes after a series of mechanical stimulation was performed, the same protocol was performed again for confirming, as shown in Fig 5A. Noxious pinching stimuli were applied to adjacent sites to avoid damage to the skin and minimize neuronal sensitization.

Contact thermal stimuli were generated using a contact heat stimulator with a contact area of $5 \times 5 \text{ mm}^2$ and applied to the same mechanical receptive field. Local skin was moisturized to aid thermal transfer on the stimulation site. Each stimulus was 30 s in duration and the inter-stimulus interval was 3 minutes. The stimulation site was maintained at $35 \text{ }^\circ\text{C}$ during the period between stimuli. The series of stimulation temperature consisted of 40, 43, 45, and 50°C , as shown in Fig 5B.

After the contact heat stimulation was done, units which were responded to noxious pinching stimulus were further tested with the force-monitoring forceps. An increasing force was applied to form a ramp stimulus in about 10 s.

Data acquisition and analysis

Neuronal activities of POm and VP were amplified with conventional amplifier, bandpass-filtered (0.3 to 300 Hz) (Grass P511, Quincy, MA, USA) displayed on an oscilloscope (Tektronix, 5111A), and an audio monitor (Grass AM8). Then the signals were fed into a 16 channel Multi-channel Neuronal Acquisition Processor System (MNAP, Plexon, Dallas, TX, USA). Real-time spike sorting was controlled through Sortclient (Plexon).

After all the experiments were done, saved waveform data were re-sorted using Offline sorter (Plexon). Different single unit can be distinguished by Principal component analysis (PCA). Re-sorted waveform data can be imported into Neuroexplorer (Nex technologies, Litteton, MA) to do further analysis.

Units were classified into different categories based on their responses to mechanical and thermal stimulations In the classification of mechanical stimulation, every single unit activity was normalized as Z scores. The 30 bins before the stimulation application were determined to be baseline period and then all bins were transformed into Z scores. After the transformation of Z scores, unit having successive

three bins above 95% confident limit during the stimulation period was identified as responsive to the stimulation. While the mechanical stimulations were applied twice, only two times of responses consistent were considered to be a “responsive” unit. Based on the criteria, units can be classified into four categories: tactile-positive/pinch-negative type, tactile-negative/pinch-positive type, tactile-positive/pinch-positive type, and tactile-negative/pinch-negative type. Differences in response categories between each group were further examined by the Chi-square test.

In the classification of contact heat stimulation, mean response to each thermal stimulus was calculated. The 30 bins before each stimulus were determined to be baseline period. Mean responses of each stimulus which was above 95 % confident limit was consider as “responsive” by using Z- scores analysis. According to the previous contact thermal studies done in rats, temperature above 44 °C seems to be a noxious heat stimulus (Bester et al., 2000; Gauriau and Bernard, 2004b). Therefore, units could be simply classified into two categories: noxious heat- negative type, which was unresponsive to 45 and 50 °C , and noxious heat- positive type, which was responsive to 45 or 50 °C .

Further analysis for coding ability was examined in mechanical and thermal stimulation. For mechanical coding ability examination, linear regression analysis was shown in the mean firing frequency and the stimulus intensity. And for thermal coding

ability, average response to each stimulus was shown in a stimulus- response curves.

Histology

After the final recording sites, electrolytic lesions (20~30 μ A for 10 s, three times) were made in the deepest channel. After withdrawing the probe, the rat was deeply anesthetized with an overdose of pentobarbital (i.p., 75 mg/kg) and perfused with physiological saline followed by 4% formaldehyde in 0.1 M phosphate buffer at pH 7.4. The brain was stored in 20% sucrose phosphate buffer (0.1 M, pH 7.4). Several days later, 50 μ m thick frozen sections were made serially in the coronal plane on a freezing microtome. After the sections stained for HRP by DAB stabilization method, they were further stained for cytochrome oxidase for nuclear demarcations analysis (Fig. 6). Sections with the kainic lesion site were stained with cresyl violet to identify the lesion extent. The lesion sites and recording tracks were documented with camera lucida drawings.

Immunohistochemistry for parvalbumin

7~8 days after kainic acid lesion, 5 rats were perfused with physiological saline followed by 4% paraformaldehyde without recordings, in order to stain for parvalbumin. Parvalbumin is a calcium binding protein which is regarded as a “transport/buffer” protein. Many previous studies have indicated that parvalbumin can act as chemical markers for GABAergic neurons in some nuclei, including ZI (Gulyas

et al., 1991; Kolmac and Mitrofanis, 1999). Therefore, we stained for parvalbumin to identify GABAergic neurons.

The brain sections were cut 30 μ m thick frozen sections serially in the coronal plane on a freezing microtome. After a brief rinse in phosphate buffer (PB; 0.1 M, pH 7.4), sections were pre-incubated with the blocking solution (0.25% triton, 5% normal serum solution) 2 hours at 4°C and then introduced in primary antiserum solution (mouse anti-rat parvalbumin; 1:3000 in 1% normal serum, 0.25% triton X-100 phosphate buffer solution) overnight at 4°C. After 3 times of rinse in PB at room temperature, sections were incubated in biotinylated secondary antibody solution (anti mouse IgG, PK-6102, Vector laboratories, Burlingame, CA; in 0.25 % triton X-100 phosphate buffer solution) for an hour, rinsed in PB three times, reacted with avidin-labeled peroxidase (ABC kit, PK-6102, Vector laboratories, Burlingame, CA) for 1 hour, and a diaminobenzidine- 30% H₂O₂ solution for 10 minutes at room temperature. After 3 times of rinses in PBS, sections were placed on gelatin-coated glass slides, air-dried, hydrated with 100% alcohol and coverslipped. A microscope with a digital camera was used to capture the images of the brain sections.

Result

I. Anterograde Tracing Study

A. Electrophysiological identification of ZI

As the microelectrode penetrating the brain tissue vertically, it would encounter VP complex first, which is very sensitive to the peripheral stimuli. And then, it would pass through a non-responsive fiber-rich region, medial lemniscal (ml). This silent zone is followed by the ZI, at which cells possessing large contralateral facial receptive fields. Many of their receptive fields even spanned the whole whisker pad. Like other somatosensory thalamic nuclei, ZI also displays topographic representations. However, the somatotopic map of ZI seems to be restricted in the upper body, the face and forelimb region. In our penetration tracts of 18 rats, none of the receptive fields were found in the lower body region. Fig 3 shows an example of responsiveness units along a ZI recording tract in coronal plane.

In the ZI, many cells displayed low-threshold type of responsiveness and many cells responded to noxious stimuli as well. Fig 2 is an example of a ZI neuron responsiveness to mechanical stimuli. The neuron showed wide-dynamic range responsiveness to mechanical stimuli, which means that the neuron responded to both innocuous and noxious stimuli.

ZI units had quite different properties from those of the VP units. First of all, ZI

units usually showed slowly adapting responses to the peripheral stimulation while VP units usually displayed rapidly adapting responses. Second, ZI units usually possessed larger cutaneous receptive fields than that of the VP units.

B. BDA injection in the ZI

Fig 7 is an example of BDA injected in the ZI facial area. The tracer injection site and spread area was very focus on the ZIV, which is mainly consist of GABAergic neurons. Fig 7C shows the labeled terminals on the level of posterior 2.5 ~ 4.3 mm referring to the bregma, as seen in the coronal sections.

Incerto-thalamic fibers primarily formed two clusters of terminals in the POM: one in the POM-VP border, and the other medially near the intralaminar nuclei. The cluster in the POM-VP border extended back from about -3 to -4 mm referring to the bregma. Another cluster which is medially near the intralaminar nuclei didn't extend back to this level. In the cluster of POM-VP border, the majority of the labeled terminals were in the range of 2 ~ 5 μ m in their longer axis, showing in Fig 7B insert.

A summary of the distribution pattern of BDA-labeled terminals of 5 rats after BDA injected into ZI is shown in Fig 8. Each color represents results from one rat. Fig 8A shows the injection site in the ZI region which responded to whiskers (n = 4) and forepaw (n = 1) stimulation. All of the tracer diffusion area was focused and restricted

in the ZI region. Label terminals were shown in Fig 8B, as seen in coronal sections referring to the bregma. Terminals were also found two clusters in the POm region ranging from -3 to -4 mm comparing to the example of Fig 7.

In addition to the POm, labeled terminals were also found in the ipsilateral side of centrolateral thalamic nucleus (CL), ventrolateral thalamic nucleus (VL), angular thalamic nucleus (AngT), laterodorsal thalamic nucleus (LD), reticular thalamic nucleus (Rt), and ZI itself. In all of the cases, labeling profile of contralateral side was not found.

We next tried to find out an input convergence area in the POm from peripheral nociceptive input and from the ZI. By reviewing the previous studies (Iwata et al., 1992; Gauriau and Bernard, 2004a), we constructed two inputs into three levels of coronal sections, as seen in Fig 9. One input is from the superficial lamina of dorsal horn, which is believed that high-threshold neurons are mainly located in, and the other is from the ZI. By constructing two inputs, we found that there is an overlapping area around the POm-VP border in the POm. In other words, there is an input convergence area in the POm.

According to the tracing results, we determined the VP-POm border area to be the main target in our recording experiments.

II. Electrophysiological Experiments

A. Lesion of ZI

An important and consistent finding of the ZI lesioning procedure was that each case injected with kainic acid showed a nearly complete destruction of the ZI. Fig 4 is an example of ZI lesion unilaterally stained with cresyl violet (A) and parvalbumin (C, D) as seen in coronal sections. One week after injection of kainic acid, a complete loss of neurons and displacement of glia cells was discernible in the lesion side. Therefore, under Nissl stain, the lesion site was deeply staining due to a highly concentration of glia cells, as shown in Fig 4A. Examining the lesion extent, we discovered the lesion area was almost restricted in the ZI in twelve rats recorded, as shown in Fig 10.

Regarding the distribution of parvalbumin-immunoreactive neurons in the ZI, almost all the neurons located in the ZIv of the contralateral side, as shown in Fig 4C. However, few parvalbumin-immunoreactive neurons were discovered in the ZIv of the lesion side, as shown in Fig 4D. The lesion analysis shows that GABAergic neurons in the ZIv, which can be seen under immunohistochemistry for parvalbumin, were lost after kainic acid lesion.

B. Response of POM and VP neurons to mechanical stimulation

In ZI lesion rats, some units responded to brushing or pinching stimuli in the ipsilateral POM. Based on our criteria, units can be classified into four categories:

tactile-positive/ pinch-negative type, tactile-negative/ pinch-positive type, tactile-positive/ pinch-positive type, and tactile-negative/ pinch-negative type. Fig 11 is an example of a POM neuron showing low-threshold responsiveness to mechanical stimuli, which was classified into tactile-positive/pinch-negative type of neurons in our classification. And Fig 12 is an example of a POM neuron showing wide-dynamic range responsiveness to mechanical stimulation, which was classified into tactile-positive/pinch-positive type of neurons. Fig 13 is another example of a POM unit recorded in naïve rat. The unit showed high-threshold responsiveness in the first trial of mechanical stimulation, while it showed no responsiveness in the second trial. This unit was therefore defined as a tactile-negative/ pinch-negative neuron.

There were 42 units recorded in the ZI lesion side of POM, 22 units recorded in the contralateral side, and 59 units in the naïve rat without lesion. Unit responses were classified into different categories, as shown in Table 1. Considering the response categories, there were significant differences between the ipsilateral to the contralateral side, and ipsilateral side to the POM of naïve animals ($p < 0.01$, Chi-square test). Units recorded in the VP complex were also categorized into different response groups, as shown in Table 2. Unlike the POM, there is no significant difference between groups. Fig 14 shows three examples recorded in different groups of VP.

Fig 15 depicts a representative plot of the ensemble responses of all units. Color scale represents the firing frequency in Z-scores. The plots show that the responses of POM in ZI lesion side were quite different to the contralateral side and the naïve animals, although there were still 1/3 units didn't respond to any mechanical stimuli. All groups of the VP displayed better responses compared to the POM in ZI lesion side.

5 pinch-positive units in the POM of the ZI-lesion side and 7 pinch-positive units in the VPM were further tested by a force-monitoring pincher. Their responses were shown in Fig 16. Linear regression analysis was made to examine the coding ability of the units. Both of the POM and VP could be found increasing function between the mean firing frequency and the stimulus intensity, as shown in Fig 17A. There is no significantly difference between the VPM and POM comparing the slopes of the linear functions and the correlation coefficients ($p > 0.05$; T-test), as shown in Fig 17B.

These results indicate that the responses to mechanical innocuous and noxious stimulations of some POM units were both revealed by ZI lesion. In contrast, VP neuronal responses to stimulation were not affected after ZI lesion. Considering the coding ability for noxious mechanical stimulation, both of the POM of the ZI lesion side and the VP of naïve animals showed increasing responses to stimulus intensity.

C. Response of POM and VP neurons to contact thermal stimulation

Responses of units to contact thermal stimulation were also categorized. According to the human subject judgments, stimuli of 45 °C and 50°C are thought to be noxious heat. Therefore, units can simply be classified into two response categories: 45 or 50 °C positive type, which was responded to noxious heat, and 45 and 50 °C negative type, which was not responded to noxious heat. Fig 18 was an example of a unit responded to 45 °C and 50 °C. Table 3 shows the response categories to thermal stimulation of all the POM units. Over 31 units recorded in the ipsilateral side of POM, 19 units were responded to 45 or 50 °C. Two units over 19 recorded in the contralateral side, and 7 units over 40 recorded in the naïve rats responded to 45 or 50 °C, respectively. There were significant differences between ZI-lesion side to the contralateral side ($p < 0.05$, Chi-square test), and ZI-lesion side to the naïve animals ($p < 0.01$, Chi-square test). However, the results of VP showed that ZI lesion was not correlated to the response categories, see Table 5. Analysis of convergency and segregation of thermal nociceptive and mechanical nociceptive inputs in POM was shown in Table 4.

Further analysis of stimulus-response curves were made in Fig 19. Stimulus-response curves of all POM (upper panel) and VP (lower panel) units which responded to noxious heat (45 °C or 50 °C) were shown in Fig 19A. The average

stimulus-response curves of POM units were shown in Fig 19B. The response pattern was no significant difference between each group ($P > 0.05$; Two-way ANOVA, Tukey test). Average curves of VP units were not shown due to the small numbers.

The results indicate that the responses of some POM units to noxious heat stimulation of some POM units were revealed by ZI lesion. In contrast, VP responses were not affected after ZI lesion. However, it seems that POM units which were responded to noxious heat didn't encode the temperature changes.

D. Cell locations

By histochemistry for cytochrome oxidase, nuclear demarcations around the POM can be clearly identified. Therefore, after penetration tract was identified by HRP-DAB method, as shown in Fig 6, cell locations can be identified under this histology processes.

Schematic diagrams shown in Fig 20 illustrate cell locations. Each symbol represents different response categories to mechanical stimulation. The diagrams show that the majority of responsiveness units were located in the POM-VP border, which is consistent to our tracing results.

Discussion

The most important findings of the present study are: (1) The massive incerto-POM projection may tonically inhibit POM tactile and nociceptive functions. (2) The hidden nociceptive POM function was revealed in ZI lesioned condition.

From our tracing studies, we found that incerto-thalamic fibers project densely to the POM in the border region to the VP, in which is convergent with peripheral nociceptive inputs. And from our electrophysiological results, POM responses to innocuous and noxious stimulation are revealed by ZI lesion. These data demonstrate that the ZI neurons may modulate the processing of nociceptive information in the POM.

Incerto-thalamic terminal field

Our tracing results showed that the ZI projects densely to the POM. Despite POM, thalamic nuclei containing terminals from ZI included ipsilateral side of centrolateral nucleus (CL), ventrolateral thalamic nucleus (VL), angular thalamic nucleus (AngT), laterodorsal thalamic nucleus (LD), reticular thalamic nucleus (Rt) and ZI itself. None of the first order thalamic nucleus of the dorsal thalamus was labeled in this study. The results are consistent to previous findings (Power et al., 1999; Bartho et al., 2002; Cavdar et al., 2006).

In all of the tracing cases in present study, focused and limited ZI injections

resulted in abundant fibers labeling within the ZI itself, which indicates the property of intranuclear connections among ZI neurons. Comparing to the Rt, another ventral thalamic nucleus giving inhibitory control to the POm, the ZI seems to have more intranuclear connections (Bartho et al., 2002). Previous data is also mentioned that there is a network of interconnections between the ZI and the higher- order thalamic nuclei on both sides of the thalamus (Power and Mitrofanis, 1999, 2001). In our studies, we also examined the labeled profiles of contralateral side. However, no labeled terminal was discovered on the contralateral side. Smaller amount of tracer deposits in the present study might be a reason for the inconsistency.

Comparing with previous data about projection distribution regions from the superficial lamina of dorsal horn (Iwata et al., 1992; Gauriau and Bernard, 2004a), we found that there is a convergent area in the POm around the VP-POm border from the peripheral nociceptive input and the ZI input. These results indicate that the region is highly involved in nociception processing in anatomical grounds. Therefore, we determined the VP-POm border area to be the main target in our electrophysiological study.

Nociceptive function of POm

From our electrophysiology study, we found that there are more POm units in the ZI lesion side responded to innocuous and noxious stimulation comparing with the

contralateral side or naïve animals, showing that some POm units may convey noxious mechanical or noxious heat information after releasing from the ZI inhibition. And the most responsive area is concentrated on the VP-POm border, as demonstrated in our anatomical tracing results.

Considering the coding ability for stimulation intensity, we found that POm units may be as good as VP units in mechanical stimulation after ZI lesion. It is now widely accepted that pain is composed of two components: sensory-discriminative and affective-motivational components (Melzack and Casey, 1968). According to the theory, discriminative information, such as stimulus intensity and location, is transmitted through the dorsal horn to the VP and eventually to the somatosensory cortex. Medial thalamus is thought to be involved in affective or motivational aspects of pain due to irregular responses to noxious stimuli and large receptive fields (Bushnell and Duncan, 1989). Therefore, in the present study, we try to test the hypothesis that POm units may release from the ZI inhibition by examination the coding ability for mechanical and thermal stimulation. We found that responses of POm units also show a linear responses to increasing stimuli intensity comparing to the VP, which is believed involving in discriminative component of pain processing. Anatomical evidence shows that lemniscal and spinothalamic system, which both consist in the discriminative system, terminate in the POm (Jones, 2007). Therefore,

we concluded that the POm might be involved in discriminative aspects of pain.

In addition to the POm recording, VP responses were also recorded in this study for positive control and for comparison purpose. From our anatomical results and previous findings, it is clear that incerto-thalamic fibers selectively terminate in the POm but VP (Power et al., 1999; Bartho et al., 2002). In the present study, we found no significant difference between tactile responsive units in the VP of the ZI lesion side versus those of the intact side, which is consistent to this connectional data.

However, there is obviously a lack of numbers in VP, which is not consistent with previous findings (Chiang et al., 2005). This may be due to the bias of the recording tracts in the present study. According to the previous anatomical findings, superficial lamina of dorsal horn would terminate more laterally and ventrally in the VP (Iwata et al., 1992; Gauriau and Bernard, 2004a). However, our penetration tracts were more medially and dorsally in order to record the POm. Therefore, bias penetration tracts might be a consequence for encountering less noxious-responsive units in VP.

Although ZI projects densely to the POm, some POm units still didn't respond to peripheral stimuli after ZI lesion. Unresponsive units in the POm after ZI lesion may represent another population of units that receive other nuclei modulation instead of ZI. Indeed, the Rt is also reported to project to the POm (Pinault and Deschenes, 1998;

Pinault, 2004). Previous reports have even demonstrated a new GABAergic pathway from anterior pretectal nucleus (APT) to the POm with ultrastructural features similar to those of ZIv afferents (Bokor et al., 2005).

Hypotheses for ZI modulation

The present study proposes that the relay of noxious inputs in the higher-order thalamic nuclei, such as POm, relies on a mechanism of disinhibition from the ZI. That is, inhibition of the inhibitory incerto-thalamic pathway. This proposal raises an issue: under what conditions is ZIv active or inactive, thus inhibiting or releasing the flow of signals through POm. There are mainly two hypotheses proposed recently.

State-dependent gating hypothesis indicates that inhibition of ZIv is mediated through brainstem cholinergic neurons that increase their firing frequency at arousal state (Trageser et al., 2006). According to this hypothesis, increasing cholinergic activity during wakefulness would suppress ZI-mediated inhibition, thereby permitting POm responses to peripheral stimuli. In support of this hypothesis, stimulation of brainstem cholinergic neurons in anesthetized animals was found to suppress excitability of ZI neurons and to enhance sensory transmission in POm (Masri et al., 2006; Trageser et al., 2006).

Another hypothesis proposed is that sensory transmission in POm is mediated by a top-down disinhibitory mechanism which is contingent on motor activity. In support

of this hypothesis, stimulation of the motor cortex was found to suppress the vibrissal responses in ZIv. An intra-incertal GABAergic circuitry was found to mediate the suppression (Urbain and Deschenes, 2007).

Both of the hypotheses described above provide proposals for POM disinhibition in intact animals. In other words, POM may convey nociceptive information in intact, awake, and free-moving animals when disinhibited from the tonic ZI control.



References

- Ahissar E, Sosnik R, Haidarliu S (2000) Transformation from temporal to rate coding in a somatosensory thalamocortical pathway. *Nature* 406:302-306.
- Alloway KD, Hoffer ZS, Hoover JE (2003) Quantitative comparisons of corticothalamic topography within the ventrobasal complex and the posterior nucleus of the rodent thalamus. *Brain Res* 968:54-68.
- Bartho P, Freund TF, Acsady L (2002) Selective GABAergic innervation of thalamic nuclei from zona incerta. *Eur J Neurosci* 16:999-1014.
- Bester H, Chapman V, Besson JM, Bernard JF (2000) Physiological properties of the lamina I spinoparabrachial neurons in the rat. *J Neurophysiol* 83:2239-2259.
- Bokor H, Frere SG, Eyre MD, Slezia A, Ulbert I, Luthi A, Acsady L (2005) Selective GABAergic control of higher-order thalamic relays. *Neuron* 45:929-940.
- Burstein R, Dado RJ, Giesler GJ, Jr. (1990) The cells of origin of the spinothalamic tract of the rat: a quantitative reexamination. *Brain Res* 511:329-337.
- Bushnell MC, Duncan GH (1989) Sensory and affective aspects of pain perception: is medial thalamus restricted to emotional issues? *Exp Brain Res* 78:415-418.
- Cavdar S, Onat F, Cakmak YO, Saka E, Yananli HR, Aker R (2006) Connections of the zona incerta to the reticular nucleus of the thalamus in the rat. *J Anat* 209:251-258.
- Chiaia NL, Rhoades RW, Bennett-Clarke CA, Fish SE, Killackey HP (1991) Thalamic processing of vibrissal information in the rat. I. Afferent input to the medial ventral posterior and posterior nuclei. *J Comp Neurol* 314:201-216.
- Chiang CY, Zhang S, Park SJ, Hu JW, Dostrovsky JO, Sessle BJ (2005) Mechanoreceptive field and response properties of nociceptive neurons in ventral posteromedial thalamic nucleus of the rat. *Thalamus & Related Systems* 3:41~51.
- Diamond ME, Armstrong-James M, Ebner FF (1992a) Somatic sensory responses in the rostral sector of the posterior group (POm) and in the ventral posterior medial nucleus (VPM) of the rat thalamus. *J Comp Neurol* 318:462-476.
- Diamond ME, Armstrong-James M, Budway MJ, Ebner FF (1992b) Somatic sensory responses in the rostral sector of the posterior group (POm) and in the ventral posterior medial nucleus (VPM) of the rat thalamus: dependence on the barrel field cortex. *J Comp Neurol* 319:66-84.
- Gauriau C, Bernard JF (2004a) A comparative reappraisal of projections from the superficial laminae of the dorsal horn in the rat: the forebrain. *J Comp Neurol* 468:24-56.
- Gauriau C, Bernard JF (2004b) Posterior triangular thalamic neurons convey

- nociceptive messages to the secondary somatosensory and insular cortices in the rat. *J Neurosci* 24:752-761.
- Gonzalez-Lima F, Helmstetter FJ, Agudo J (1993) Functional mapping of the rat brain during drinking behavior: a fluorodeoxyglucose study. *Physiol Behav* 54:605-612.
- Gulyas AI, Toth K, Danos P, Freund TF (1991) Subpopulations of GABAergic neurons containing parvalbumin, calbindin D28k, and cholecystokinin in the rat hippocampus. *J Comp Neurol* 312:371-378.
- Guy N, Chalus M, Dallel R, Voisin DL (2005) Both oral and caudal parts of the spinal trigeminal nucleus project to the somatosensory thalamus in the rat. *Eur J Neurosci* 21:741-754.
- Hermanson O, Hallbeck M, Blomqvist A (1995) Preproenkephalin mRNA-expressing neurones in the rat thalamus. *Neuroreport* 6:833-836.
- Iwata K, Kenshalo DR, Jr., Dubner R, Nahin RL (1992) Diencephalic projections from the superficial and deep laminae of the medullary dorsal horn in the rat. *J Comp Neurol* 321:404-420.
- Jones EG (2007) *The thalamus*, second Edition. New York: Cambridge University Press.
- Kim U, Gregory E, Hall WC (1992) Pathway from the zona incerta to the superior colliculus in the rat. *J Comp Neurol* 321:555-575.
- Kolmac C, Mitrofanis J (1999) Distribution of various neurochemicals within the zona incerta: an immunocytochemical and histochemical study. *Anat Embryol (Berl)* 199:265-280.
- Lavallee P, Urbain N, Dufresne C, Bokor H, Acsady L, Deschenes M (2005) Feedforward inhibitory control of sensory information in higher-order thalamic nuclei. *J Neurosci* 25:7489-7498.
- Masri R, Bezdudnaya T, Trageser JC, Keller A (2008) Encoding of stimulus frequency and sensor motion in the posterior medial thalamic nucleus. *J Neurophysiol* 100:681-689.
- Masri R, Trageser JC, Bezdudnaya T, Li Y, Keller A (2006) Cholinergic regulation of the posterior medial thalamic nucleus. *J Neurophysiol* 96:2265-2273.
- Melzack R, Casey KL, eds (1968) *Sensory, motivational and central control determinants of pain: a new conceptual model.* : Thomas, Springfield III.
- Nicolelis MA, Chapin JK, Lin RC (1995) Development of direct GABAergic projections from the zona incerta to the somatosensory cortex of the rat. *Neuroscience* 65:609-631.
- Nicolelis MAL, Chapin JK, Lin RCS (1992) Somatotopic maps within the zona incerta relay parallel GABAergic somatosensory pathways to the neocortex,

- superior colliculus, and brainstem. *Brain Res* 577:134-141.
- Paxinos G, Watson C, eds (1998) *The rat brain: in stereotaxic coordinates.*, 4 Edition: Academic Press.
- Pinault D (2004) The thalamic reticular nucleus: structure, function and concept. *Brain Res Brain Res Rev* 46:1-31.
- Pinault D, Deschenes M (1998) Projection and innervation patterns of individual thalamic reticular axons in the thalamus of the adult rat: a three-dimensional, graphic, and morphometric analysis. *J Comp Neurol* 391:180-203.
- Power BD, Mitrofanis J (1999) Evidence for extensive inter-connections within the zona incerta in rats. *Neurosci Lett* 267:9-12.
- Power BD, Mitrofanis J (2001) Zona incerta: Substrate for contralateral interconnectivity in the thalamus of rats. *J Comp Neurol* 436:52-63.
- Power BD, Kolmac CI, Mitrofanis J (1999) Evidence for a large projection from the zona incerta to the dorsal thalamus. *J Comp Neurol* 404:554-565.
- Trageser JC, Keller A (2004) Reducing the uncertainty: gating of peripheral inputs by zona incerta. *J Neurosci* 24:8911-8915.
- Trageser JC, Burke KA, Masri R, Li Y, Sellers L, Keller A (2006) State-dependent gating of sensory inputs by zona incerta. *J Neurophysiol* 96:1456-1463.
- Urbain N, Deschenes M (2007) Motor cortex gates vibrissal responses in a thalamocortical projection pathway. *Neuron* 56:714-725.
- Yu C, Derdikman D, Haidarliu S, Ahissar E (2006) Parallel thalamic pathways for whisking and touch signals in the rat. *PLoS Biol* 4:e124.

Tables and Figures

Table 1: Response categories to mechanical stimulation of the POm units.

Response Category	Unit number of POm		Naïve rat
	ZI-lesion side	Contralateral side	
Tactile⁺ Pinch⁺	6 (10 %)	0	0
Tactile ⁻ Pinch ⁺	10 (17 %)	0	1 (2 %)
Tactile⁺ Pinch⁻	13 (22 %)	3 (9 %)	6 (10 %)
Tactile ⁻ Pinch ⁻	30 (51 %)	29 (91 %)	52 (88%)
Total	59	32	59

Significant differences were between the ZI-lesion side to the contralateral side, and ZI-lesion side to the POm of naïve animals ($p < 0.01$, chi-square test).

Table 2: Response categories to mechanical stimulation of the VP units.

Response Category	Unit number of VP		Naïve rat
	ZI-lesion side	Contralateral side	
Tactile⁺ Pinch⁺	1 (3 %)	0	3 (5 %)
Tactile ⁻ Pinch⁺	2 (7 %)	0	8 (14 %)
Tactile⁺ Pinch⁻	12 (44 %)	11 (78 %)	19 (35 %)
Tactile ⁻ Pinch ⁻	12 (44 %)	3 (21 %)	24 (44 %)
Total	27	14	54

No significant difference among groups (Chi-square test).

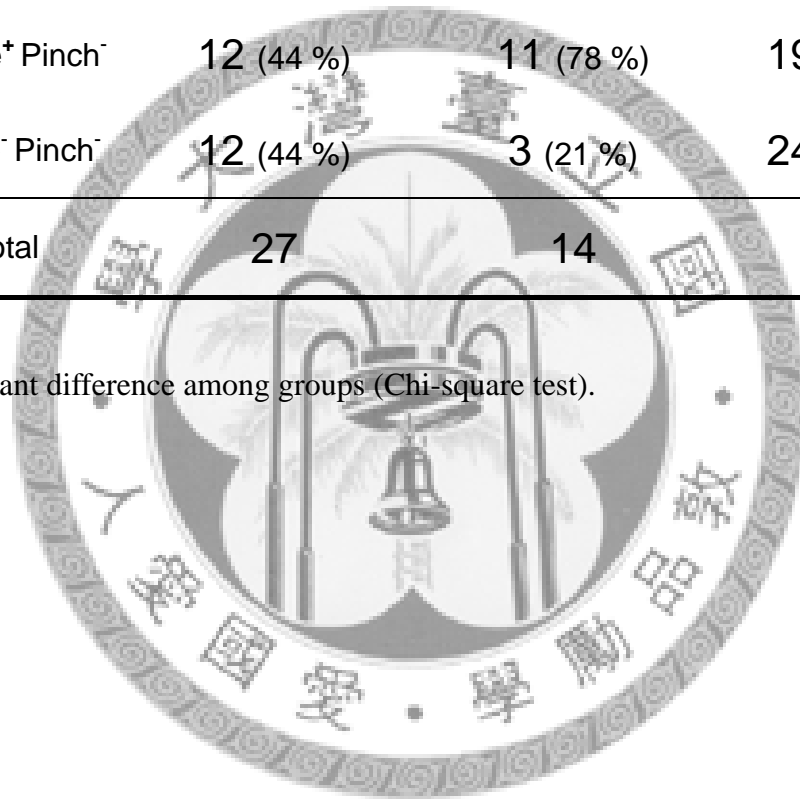


Table 3: Response categories to contact heat stimulation of the POM units.

Response Category	Unit number of POM		
	ZI-lesion side	Contralateral side	Naïve rat
Heat ⁺	14 (45 %)	3 (16 %)	10 (22 %)
Heat ⁻	17 (55 %)	16 (84 %)	35 (78 %)
Total	31	19	45

Significant differences were between the ZI-lesion side to the contralateral side, and ZI-lesion side to the POM of naïve animals ($p < 0.05$, chi-square test).

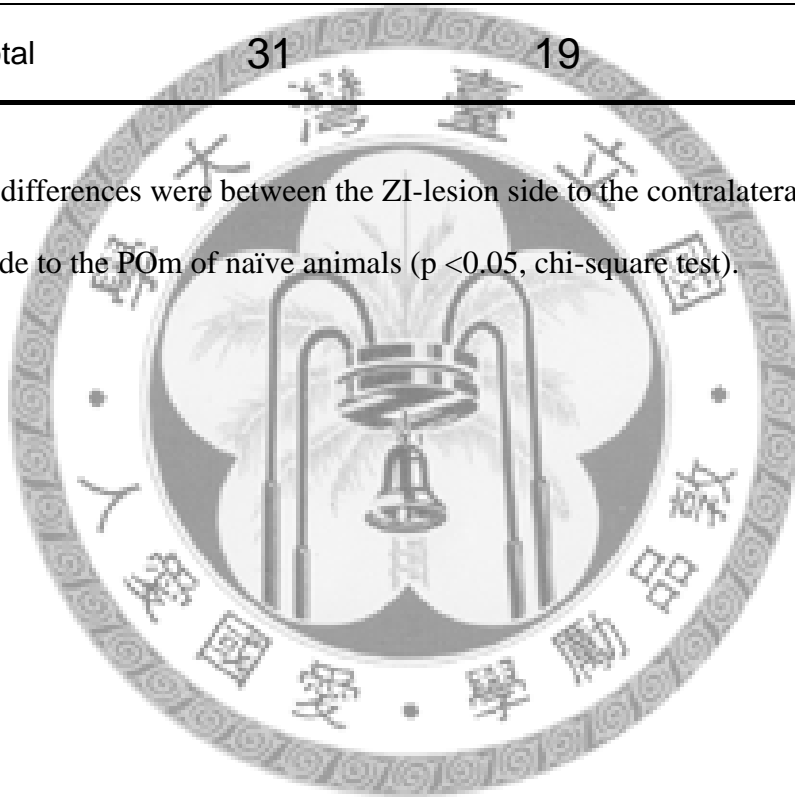


Table 4: Converge and segregation of thermal nociceptive and mechanical nociceptive inputs in POM.

Response Category	Unit number of POM		Naïve rat
	ZI-lesion side	Contralateral side	
Heat ⁺ Pinch ⁺	3 (9 %)	0	1 (2 %)
Heat ⁺ Pinch ⁻	7 (22 %)	3 (16 %)	3 (8 %)
Heat ⁻ Pinch ⁺	0	0	0
Heat ⁻ Pinch ⁻	21 (67 %)	15 (83 %)	34 (89 %)
Total	31	18	38

Mechanical and thermal stimulations were both tested in the units of this table.

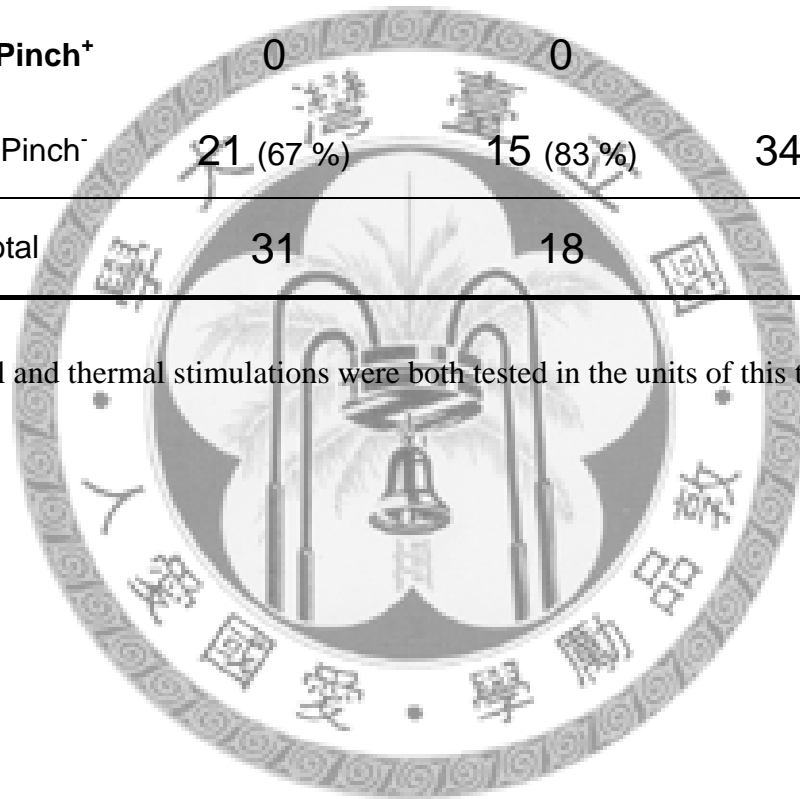
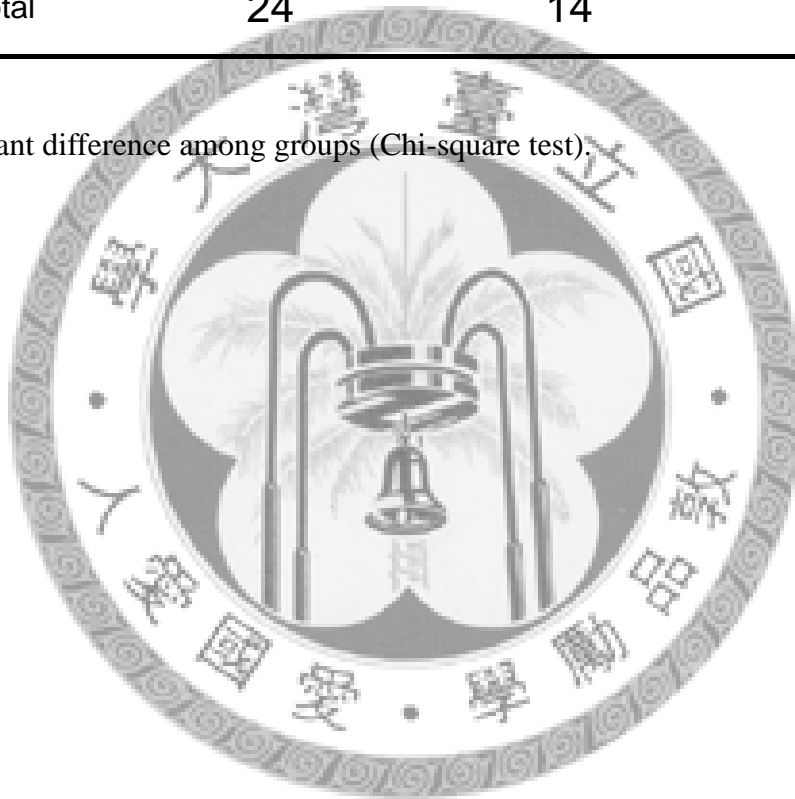


Table 5: Response categories to contact heat stimulation of the VP units.

Response Category	Unit number of VP		Naïve rat
	ZI-lesion side	Contralateral side	
Heat ⁺	1 (4 %)	1 (7 %)	2 (7 %)
Heat ⁻	23 (96 %)	13 (93 %)	28 (93 %)
Total	24	14	30

No significant difference among groups (Chi-square test).



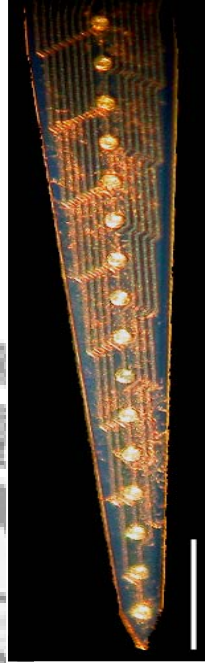
A**B**

Figure 1: A 16-channel Michigan probe used in the electrophysiology experiments. **A:** Appearance of the electrode. **B:** An enlarged view of the tip of the electrode. Distance between each recording site is $50 \mu\text{m}$. Scale bar in A: 5 mm, and in B: $100 \mu\text{m}$.

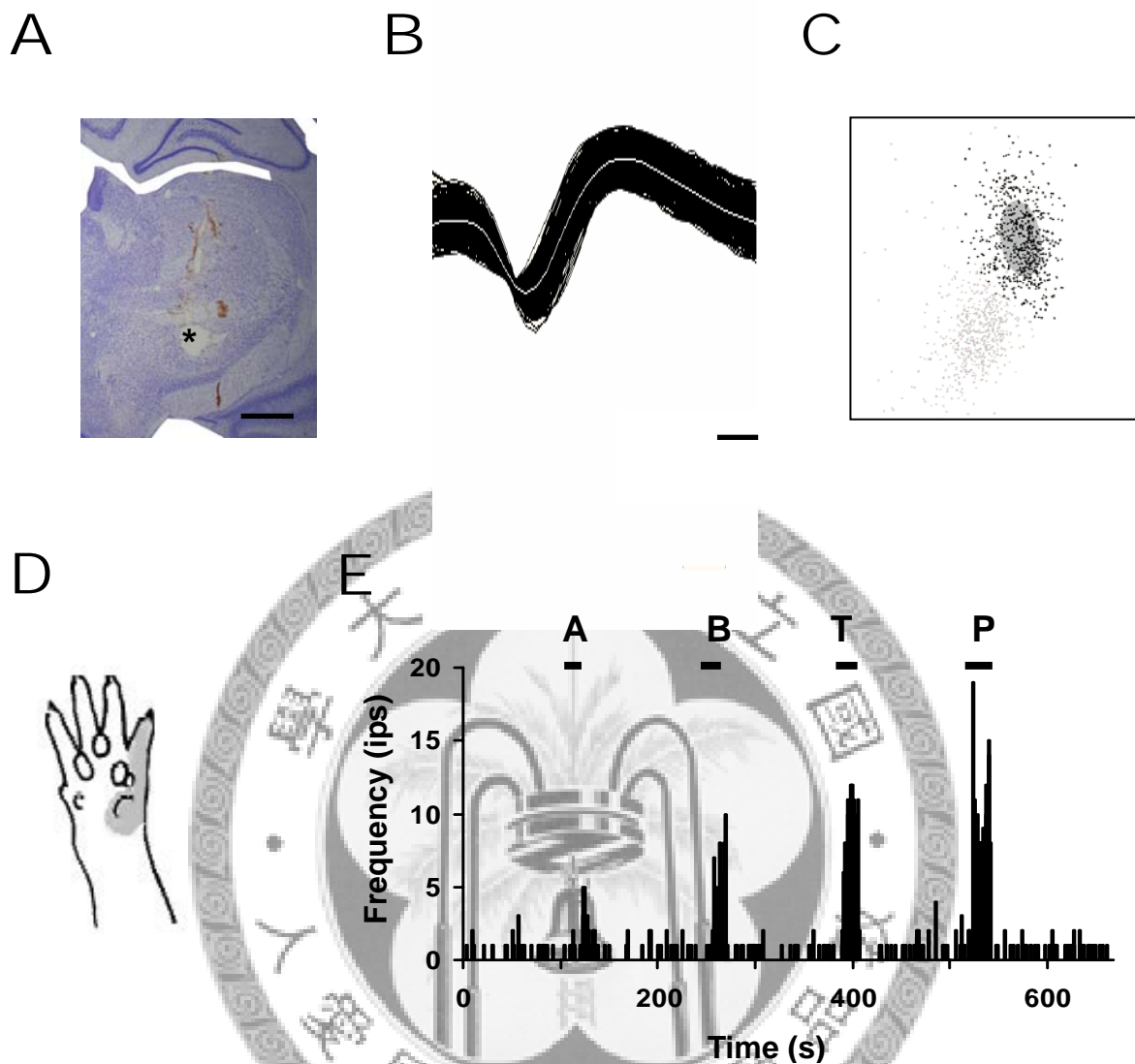


Figure 2: An example of a ZI neuron showing wide-dynamic range responsiveness to mechanical stimulation. **A:** Nissl-stained coronal section showing an electrolytic lesion (asterisk) at the recording site in ZI. **B:** Cumulative waveforms of the neuron. **C:** A 3D view of cluster analysis with PC1-PC2-PC3 plot of spikes of this neuron (black cluster). **D:** The receptive field (gray area) of this neuron. **E:** The responses of this neuron to mechanical stimuli (A: airpuff, B: brush, T: tapping, and P: pinch). Scale bar in A: 1 mm, and in B: 100 μ s. Bin size in E: 1 s.

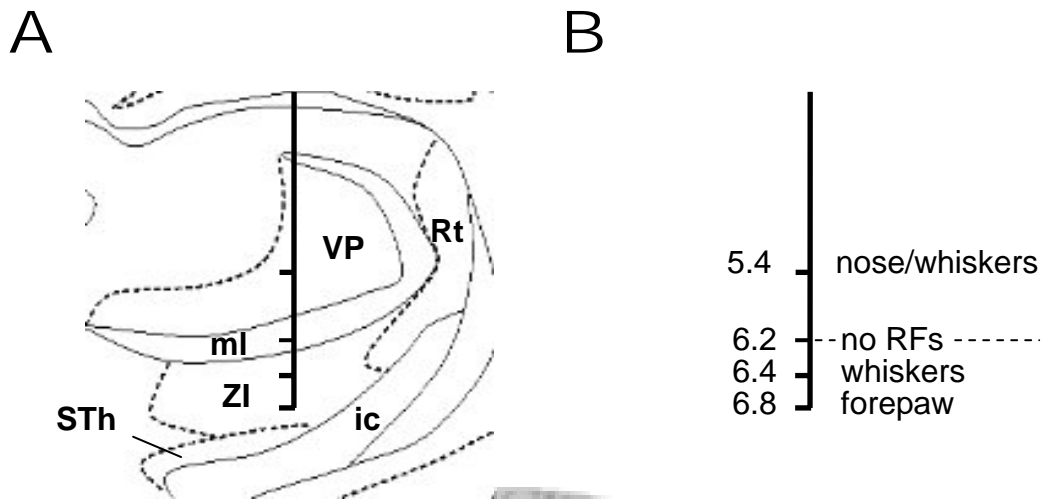


Figure 3: An example of responsiveness units along a ZI recording tract at the level of P 4 mm and L 2.5 mm referring to the bregma. **A:** The anatomical relationship around the ZI at the level of electrode penetration site. **B:** Depths of the locations of units encountered and their respective receptive fields. The dashed line separates receptive fields observed in the VP (above the dashed line) and the ZI (below the dashed line). ic, internal capsule; ml, medial lemniscus; Rt, reticular thalamic nucleus; STh, subthalamic nucleus; VP, ventral posterior nucleus; ZI, Zona incerta; No RFs: no prominent receptive field was observed. Scale bar: 0.5 cm.

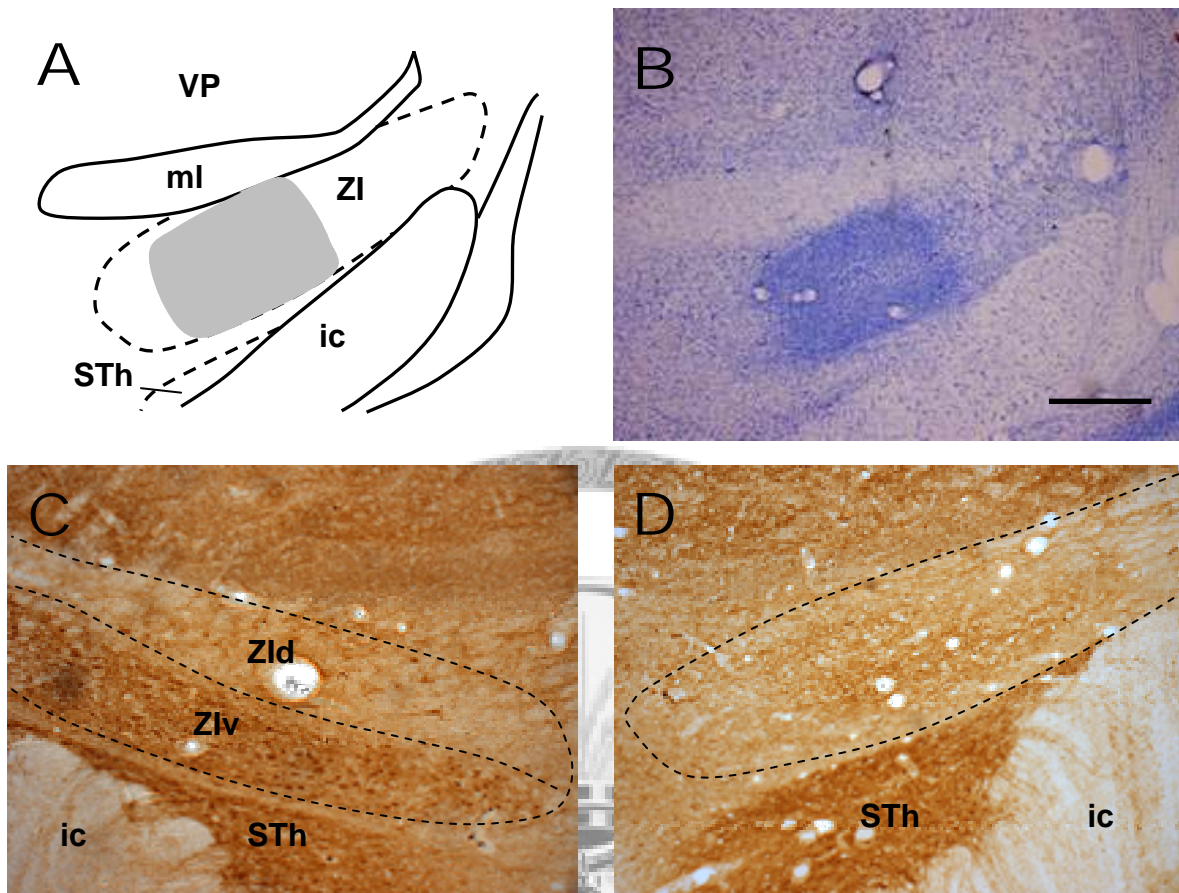
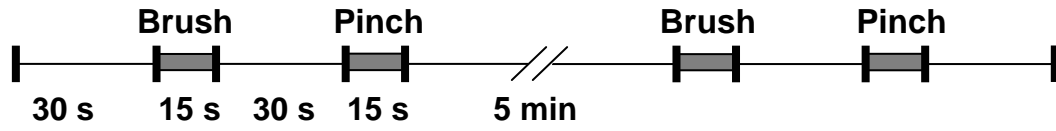


Figure 4: Coronal section stained with cresyl violet (**B**) and another example immunohistochemistry for parvalbumin (**C, D**) one week after kainic acid lesions of the ZI unilaterally. A complete loss of neurons and gliosis was discernible at the lesion side (**B, D**). **A**: The camera lucida drawing illustrates the anatomical relationship around the ZI and the extent of the lesions (gray area). **C**: The contralateral side of the ZI can be distinguished to the dorsal (ZId) and the ventral portion (ZIv) by immunohistochemistry for parvalbumin. Scale bar in A and B: 500 μ m; in C and D: 250 μ m. ZId: dorsal sector of Zona incerta; ZIv: ventral sector of Zona incerta. See other abbreviations in Figure 3 legend.

A



B

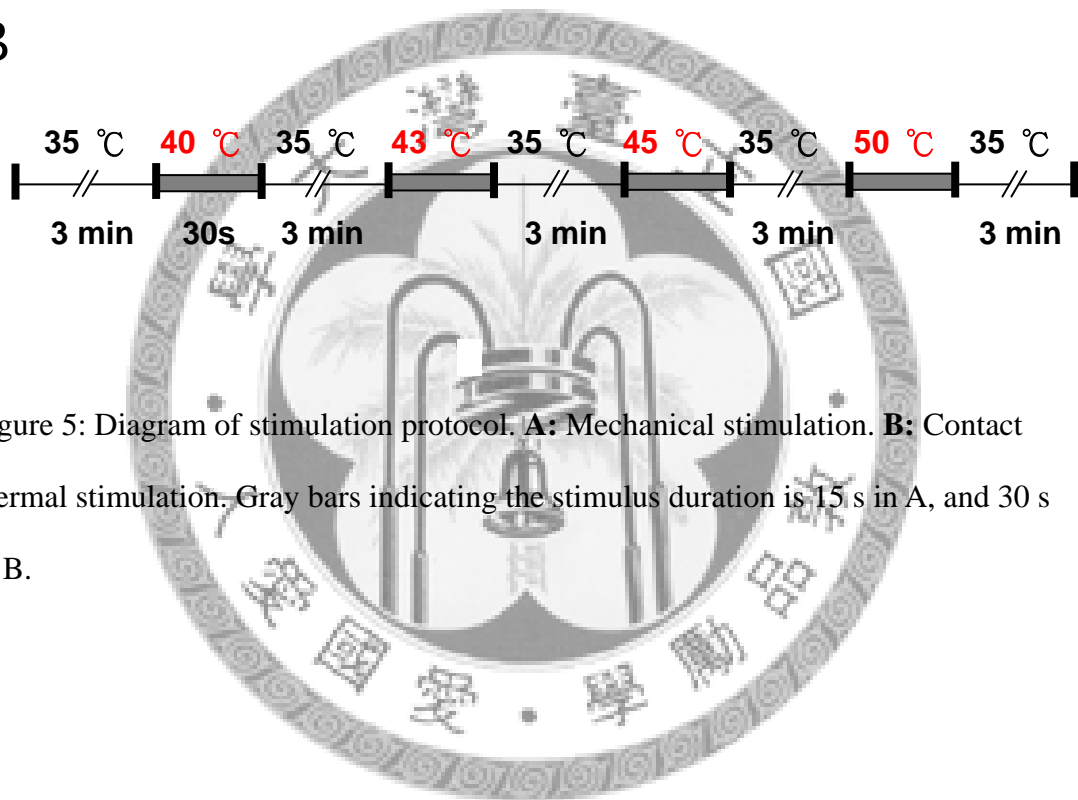


Figure 5: Diagram of stimulation protocol. **A:** Mechanical stimulation. **B:** Contact thermal stimulation. Gray bars indicating the stimulus duration is 15 s in A, and 30 s in B.

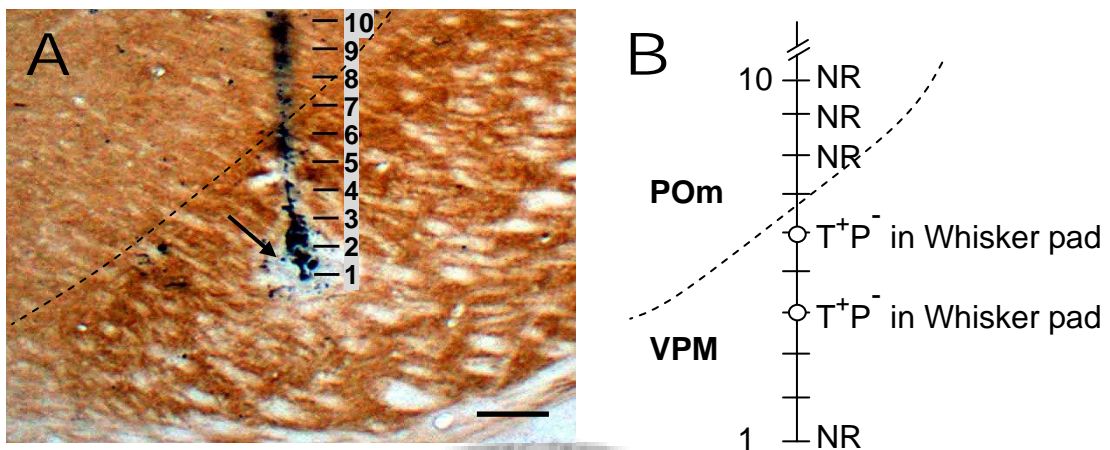


Figure 6: **A:** An example of the Michigan probe penetration tract (arrow) in a cytochrome oxidase (CO) stained coronal section. Arrow indicates the electrolytic lesion at the deepest recording site. **B:** Response category of each unit of the channel which is represented in A. The dashed line separates the densely CO immunoreactive VP (below the dashed line) and the lightly CO immunoreactive POm (above the dashed line). Scale bar in A: 200 μ m. POm, posterior medial thalamic nucleus; VP, ventral posterior nucleus; NR, unit not responsive to any of the stimuli tested. T^+P^- : Tactile positive, pinch negative unit.

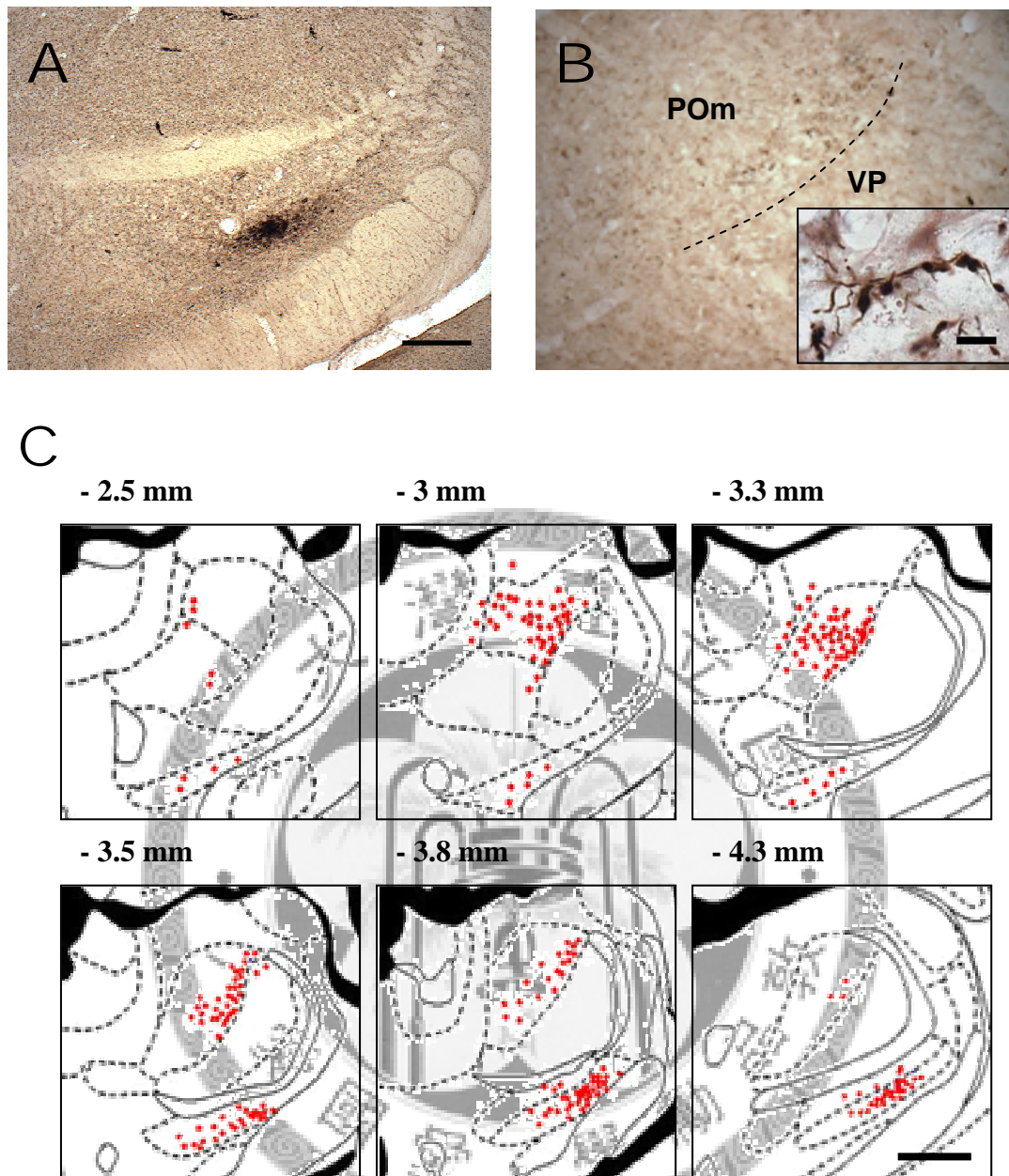


Figure 7: **A:** One example of BDA injected in the ZI whiskers area. Photomicrograph of a coronal section shows the injection site. **B:** Photomicrograph of BDA-labeled terminals in the ipsilateral POm. The dashed line separates the POm and the VP. Amplified terminals boutons are shown in the insert. **C:** Coronal planes showing the distribution of BDA-labeled terminals in the ipsilateral thalamus. Scale bar in A: 200 μ m, in B: 100 μ m, in B insert: 2 μ m, and in C: 0.5 cm. See figure 3 legend for other abbreviations.

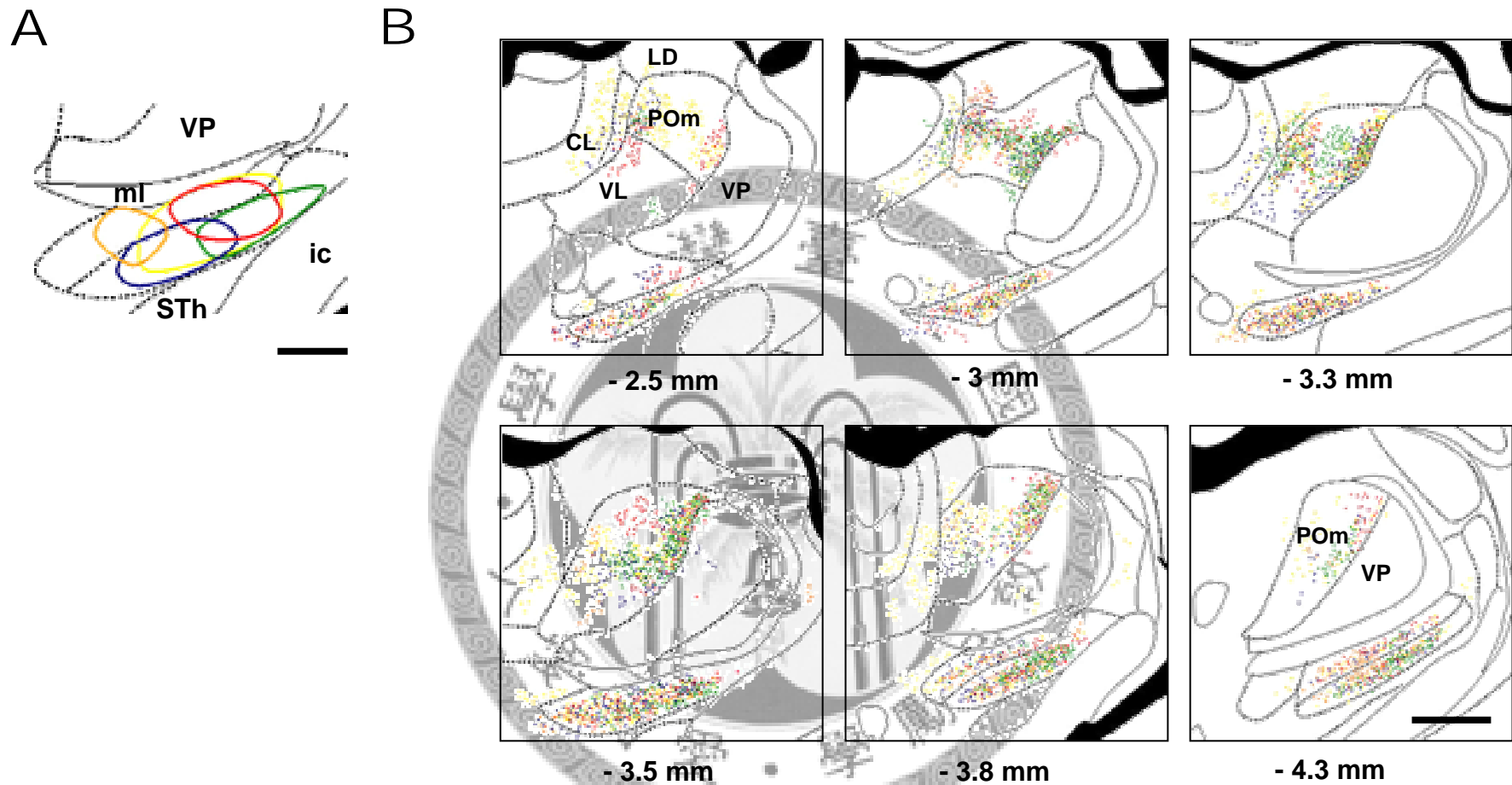
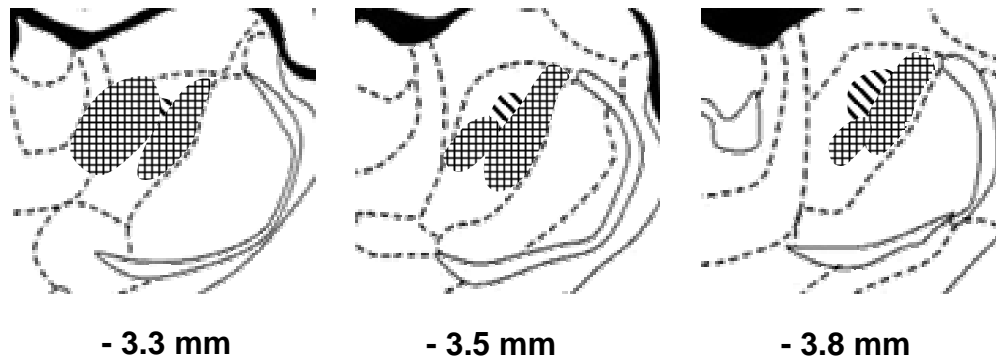
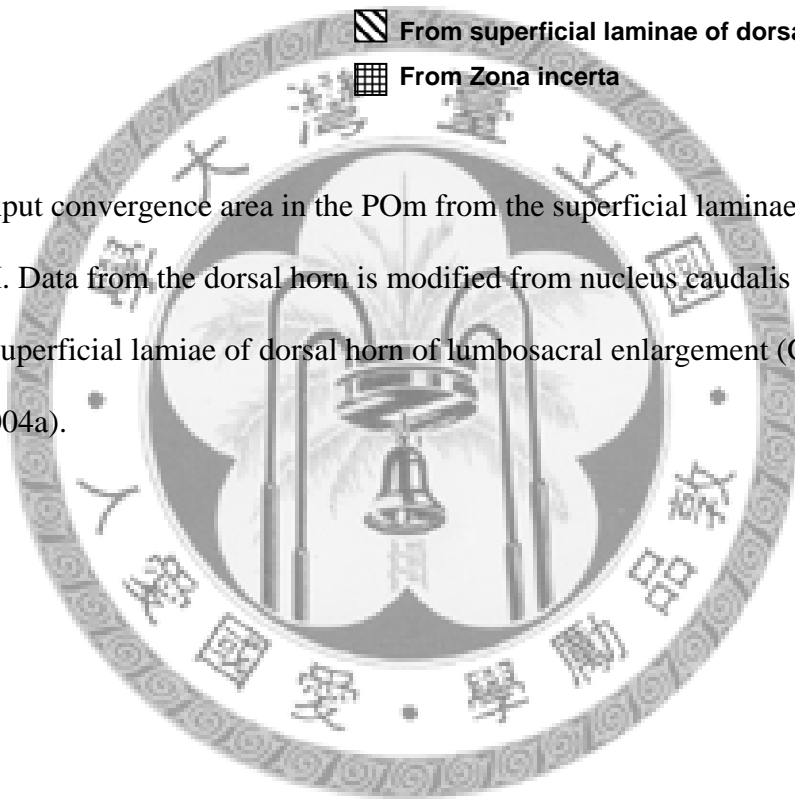


Figure 8: Summary of the labeled terminals distributions after BDA injected into the ZI whiskers ($n = 4$) and forepaw ($n = 1$) regions. **A:** BDA injection sites in the ZI. **B:** Color-coded terminal fields. Each color represents results from one rat. The numerical numbers in figure B are anteroposterior stereotaxic coordinates of the respective coronal sections relative to bregma. Scale bar in A: $200 \mu\text{m}$, and in B: 0.5 cm . See figure 3 legend for abbreviations.



From superficial laminae of dorsal horn
 From Zona incerta

Figure 9: Input convergence area in the POM from the superficial laminae of dorsal horn and ZI. Data from the dorsal horn is modified from nucleus caudalis (Iwata et al., 1992) and superficial laminae of dorsal horn of lumbosacral enlargement (Gauriau and Bernard, 2004a).



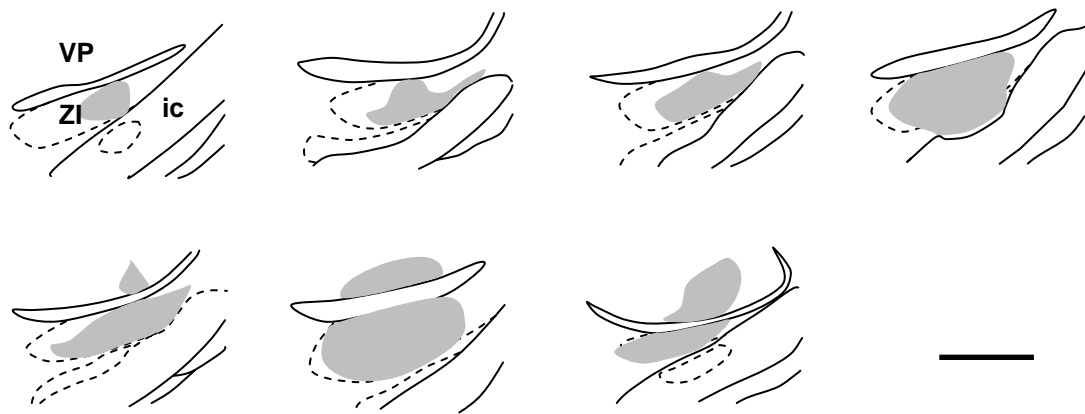
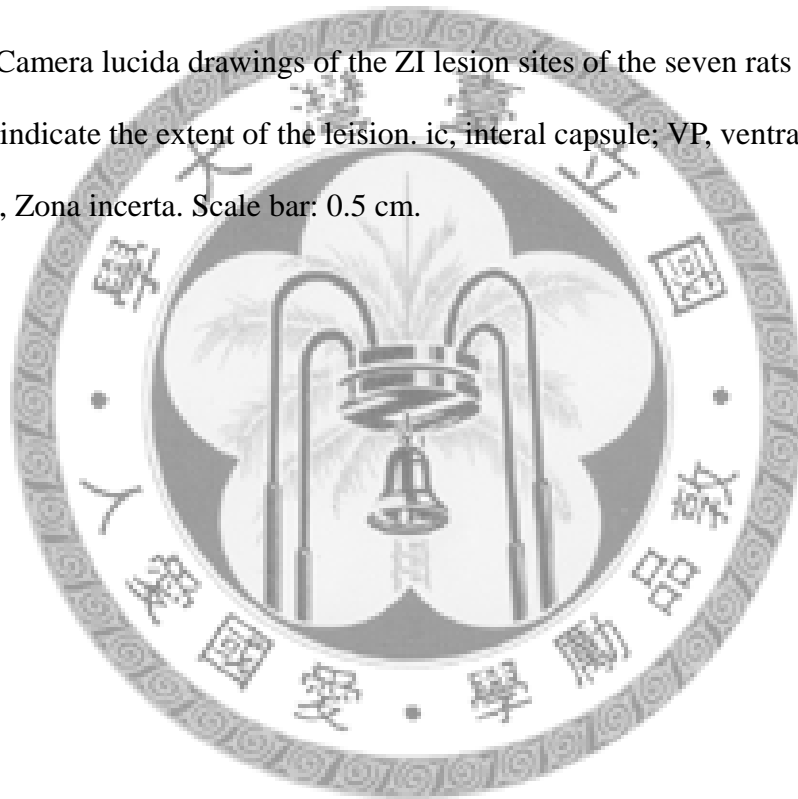


Figure 10: Camera lucida drawings of the ZI lesion sites of the seven rats recorded. Gray areas indicate the extent of the lesion. ic, internal capsule; VP, ventral posterior nucleus; ZI, Zona incerta. Scale bar: 0.5 cm.



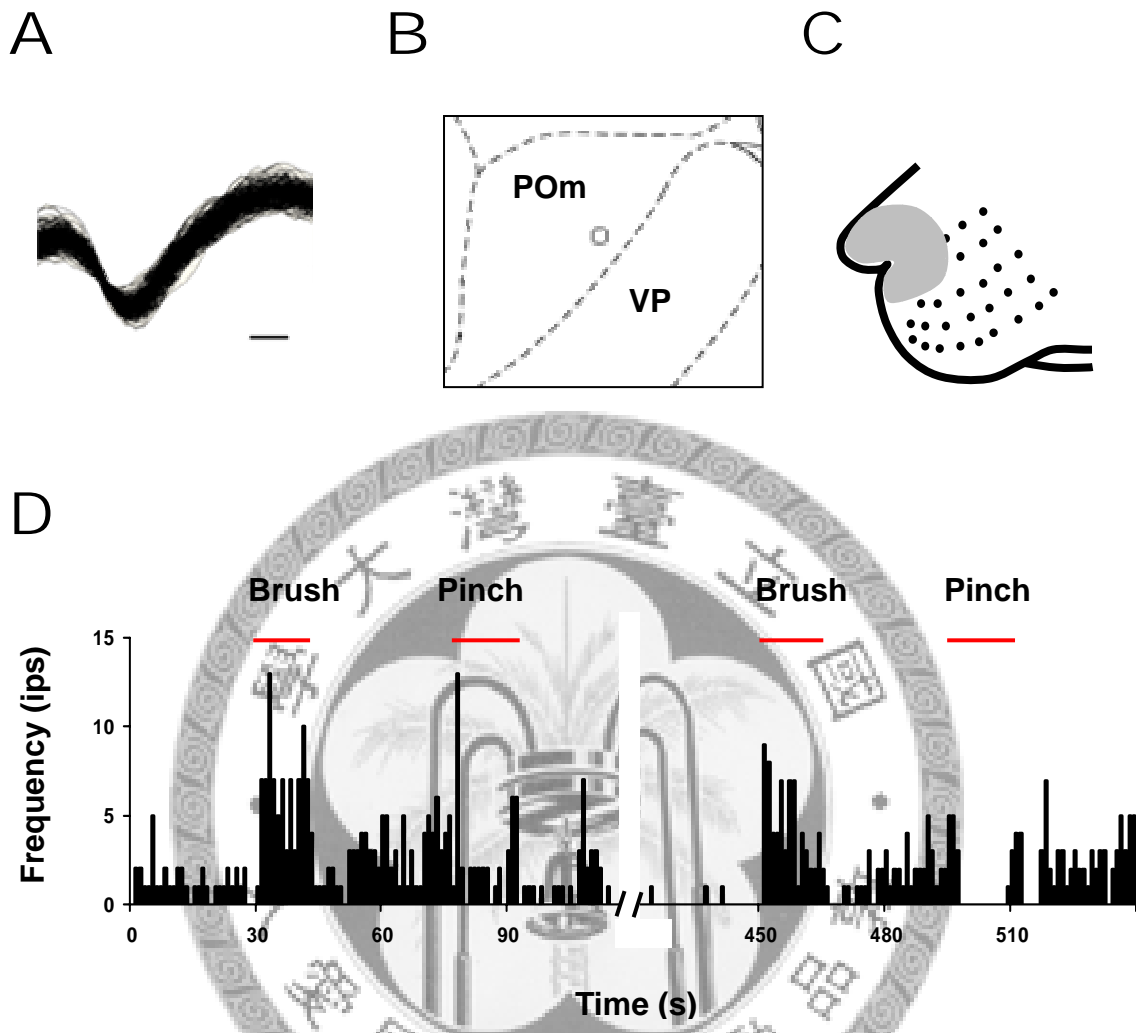


Figure 11: An example of a POm neuron showing low-threshold responsiveness to mechanical stimulations. **A**: Cumulative waveforms of the neuron. **B**: The location of the unit. **C**: The receptive field (gray area) of this neuron. **D**: The responses of this neuron to mechanical stimuli. Scale bar in A: 100 μ s. Bin size in D: 1 s.

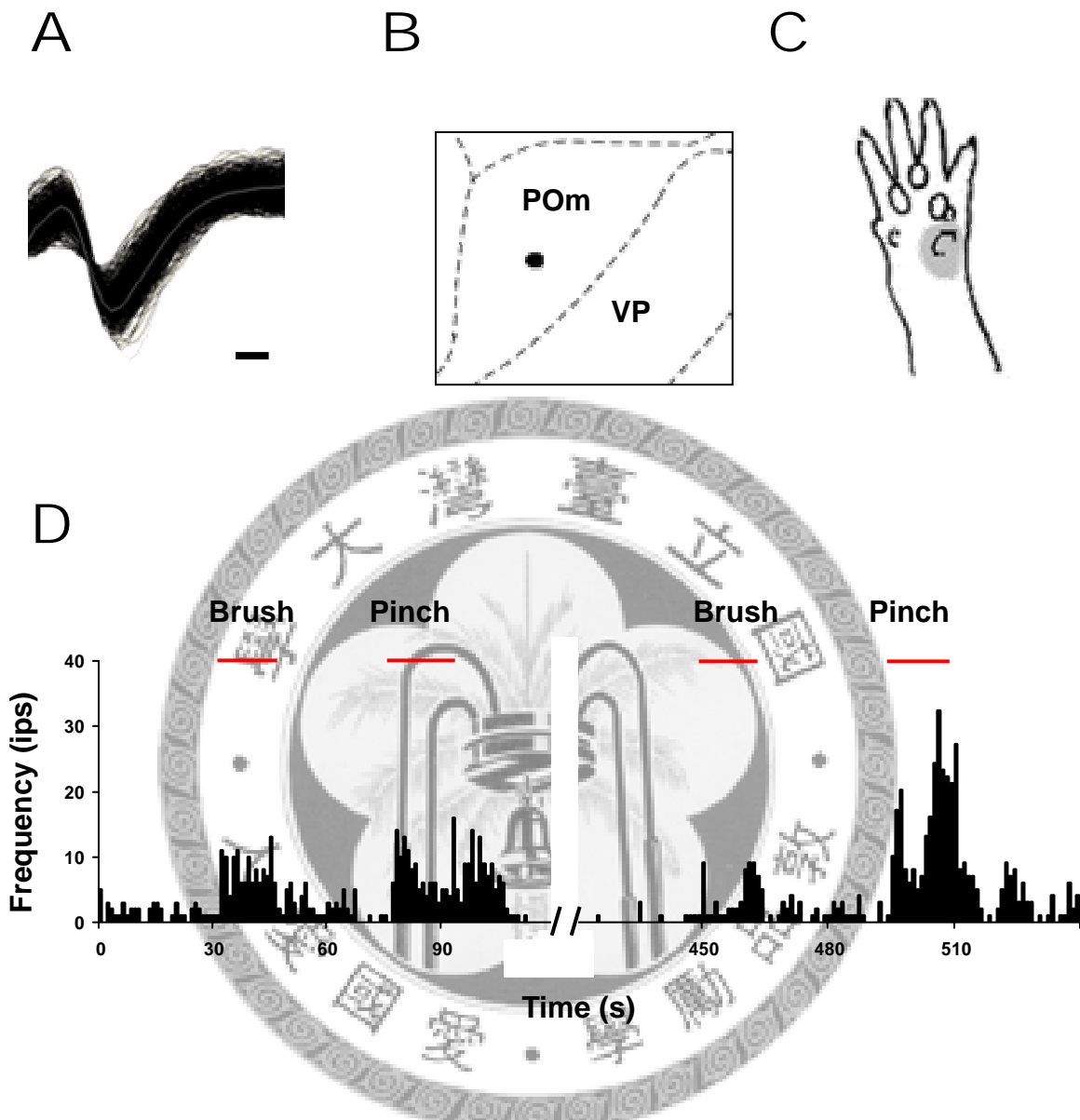


Figure 12: An example of a POm neuron showing wide-dynamic range responsiveness to mechanical stimulations. **A:** Cumulative waveforms of the neuron. **B:** The location of the unit. **C:** The receptive field (gray area) of this neuron. **D:** The responses of this neuron to mechanical stimuli. Scale bar in A: 100 μ s. Bin size in D: 1 s.

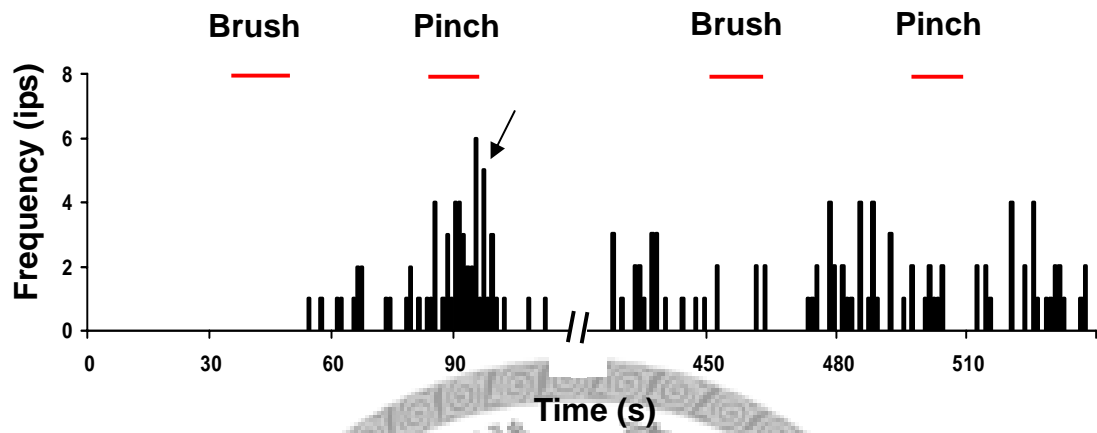
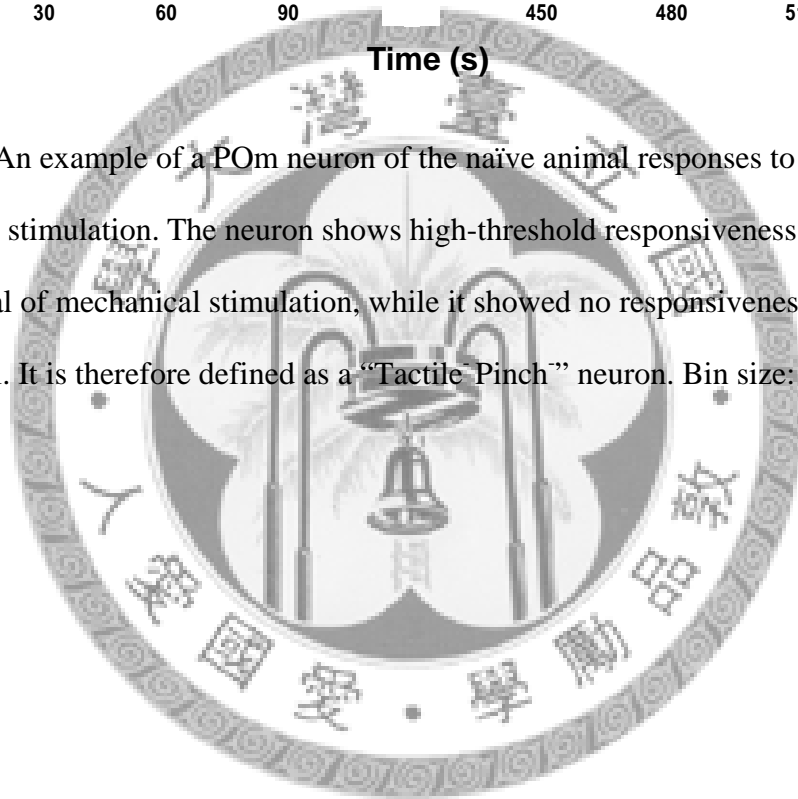


Figure 13: An example of a POm neuron of the naïve animal responses to two trials of mechanical stimulation. The neuron shows high-threshold responsiveness (arrow) to the first trial of mechanical stimulation, while it showed no responsiveness to the second trial. It is therefore defined as a “Tactile Pinch” neuron. Bin size: 1 s.



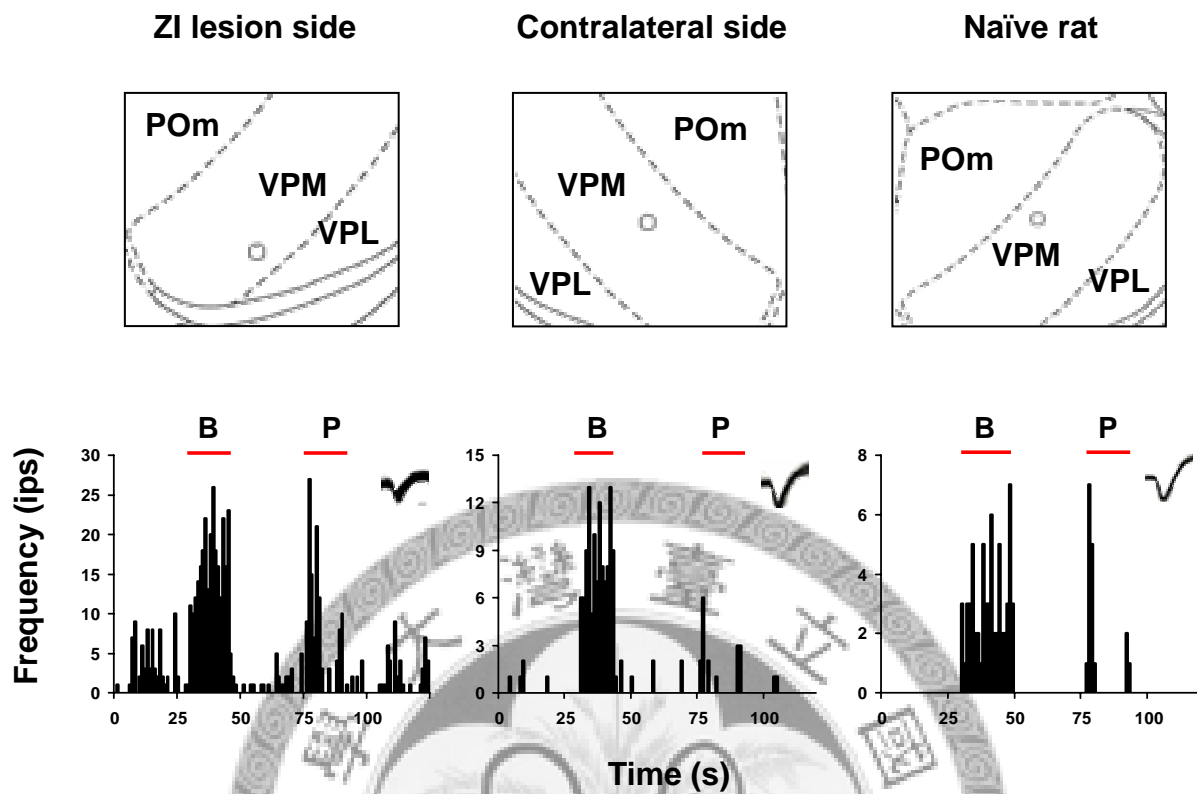


Figure 14: Response properties of the VP units with or without the ZI lesion. Left panel represents a unit recorded in the VP with the ZI lesion ipsilaterally, middle panel represents one recorded in the contralateral side, and right panel represents the other one recorded in the VP without the ZI lesion. The units locations are shown above and cumulative waveforms are shown in the insert. Scale bar: 100 μ s. B: brush, and P: pinch.

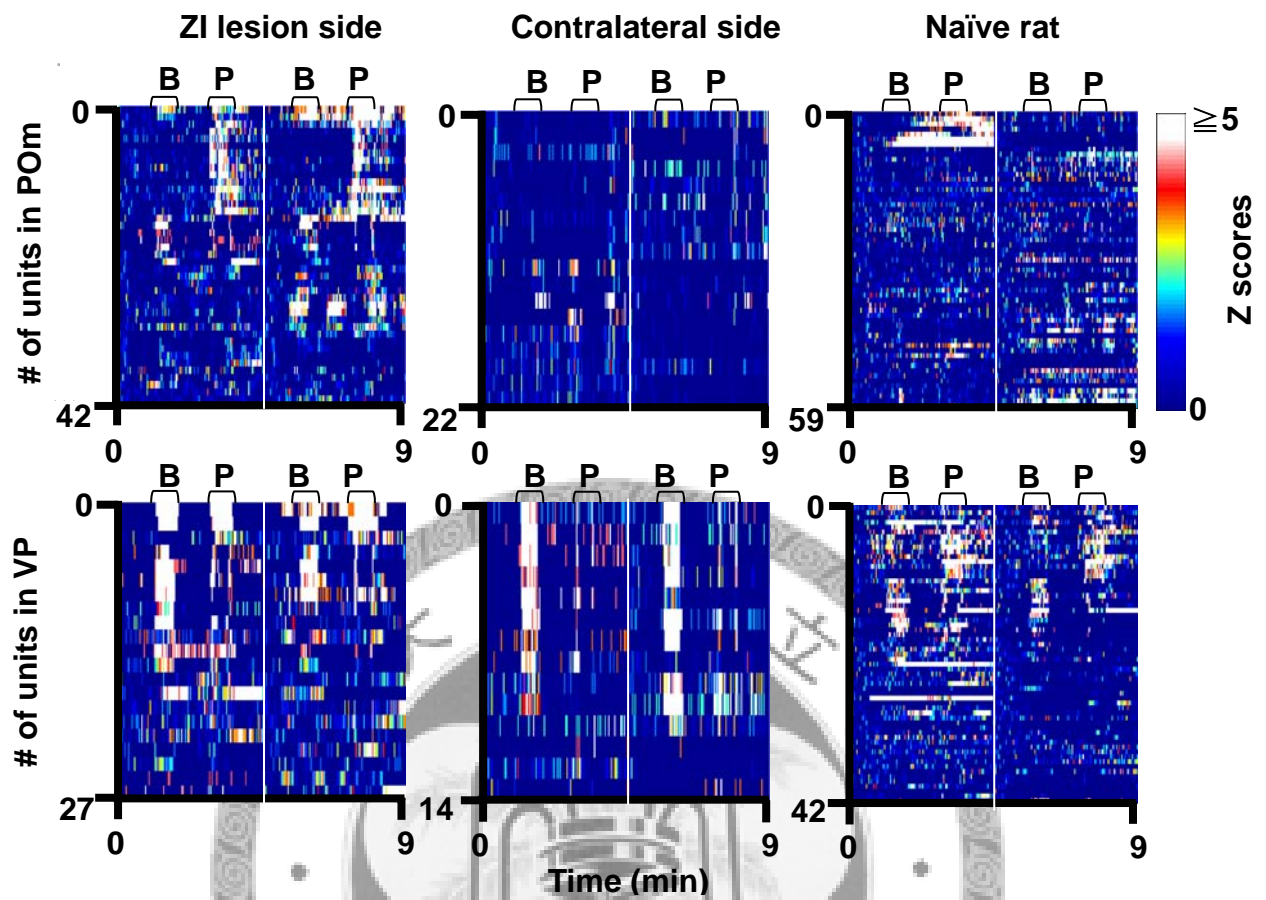


Figure 15: Ensemble responses of all units to the mechanical stimulation. Upper plots from right to left were recorded in POm of ZI-lesion side, contralateral side, and naïve animal respectively. Lower plots from right to left were recorded in VP. White lines indicate the 5 min interval between two times of trials. Color scale represents the firing frequency in z-scores. B: brush, and P: pinch.

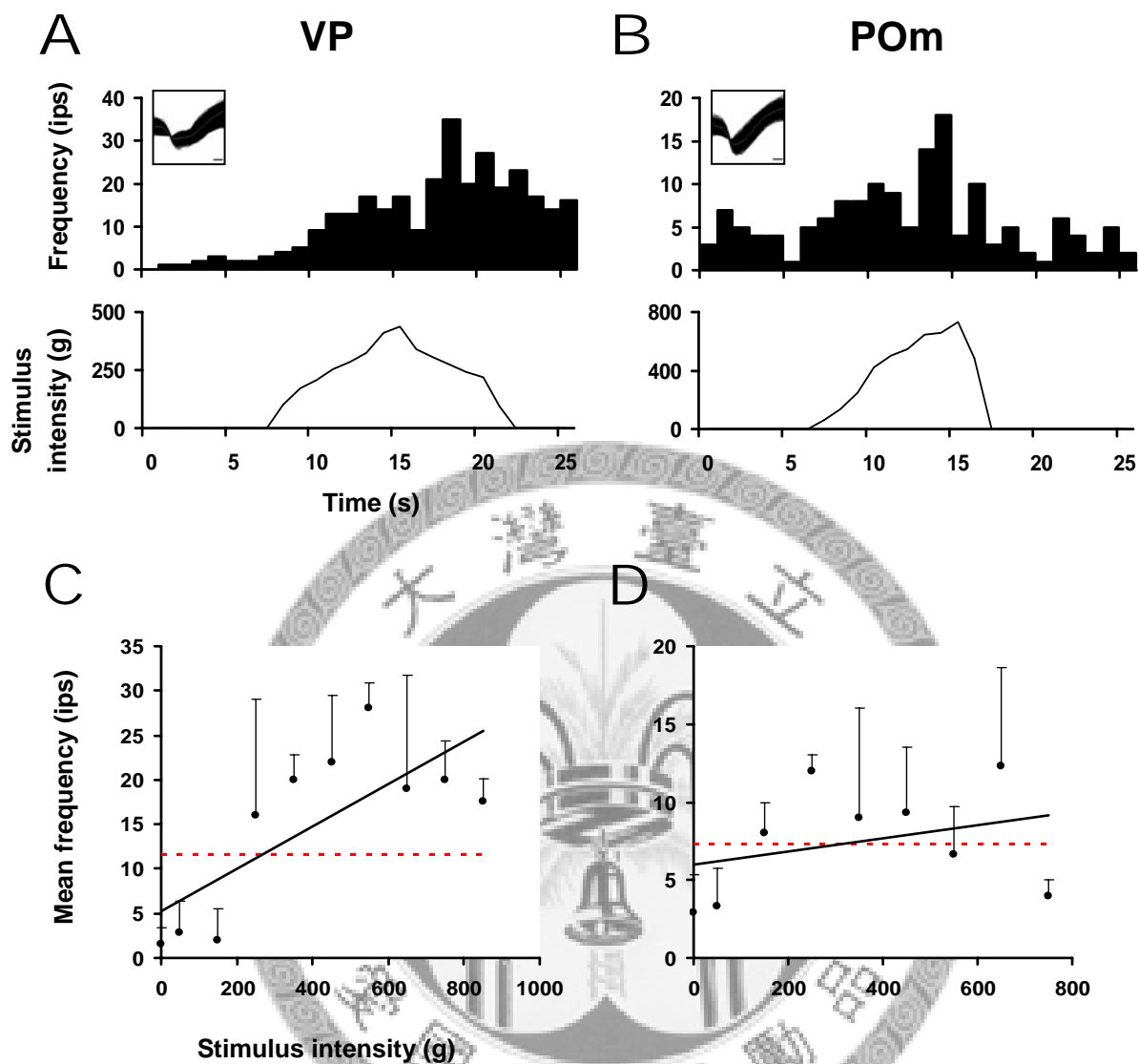


Figure 16: Examples of “Tactile Pinch⁺” VP (A, C) and POm (B, D) units responded to a ramp pinch stimulus. The unit responses were shown as a rate histogram (A, B) on the upper panels, and the stimulus intensity were shown on the lower panels. Linear regression analysis was shown in C and D. Cumulative waveforms and a 3D view of PCA analysis of spikes of the units were shown in the inserts. Dashed line indicated the 95 % confident limit which determine the threshold of unit. Scale bar in inserts of waveform: 100 μ s. Bin size in A and B: 1 s. Error bars indicates standard deviation of the mean.

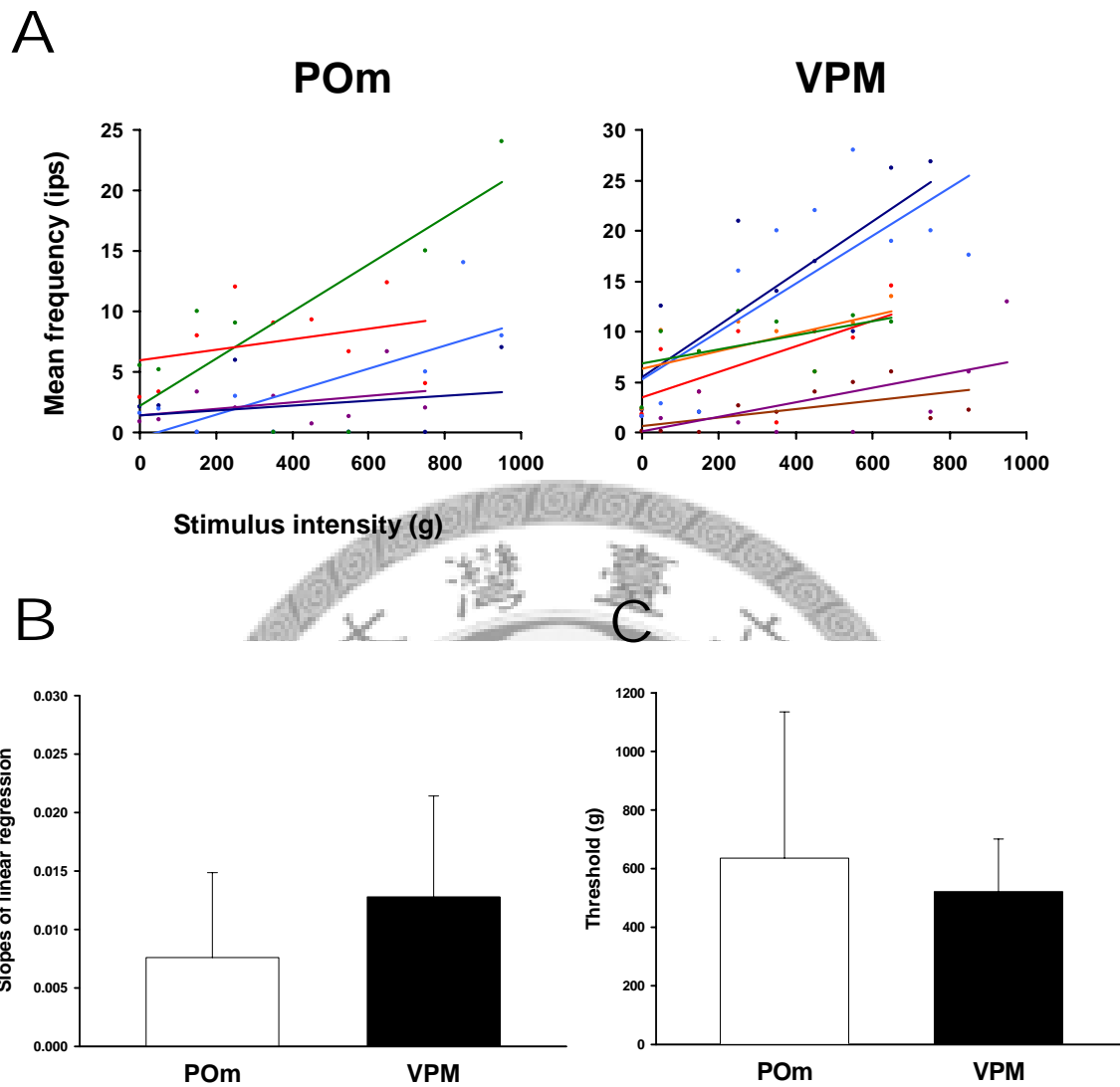


Figure 17: **A:** Linear regression analysis of 5 units recorded in the POm of the ZI-lesion side and 7 units in the VPM. An increasing function could be shown in the mean firing frequency and the stimulus intensity. There is no significant difference between the VPM and POm comparing the slopes of the linear functions (**B**) and the threshold (**C**). ($p > 0.05$; t-test) Error bars indicate standard deviation of the mean.

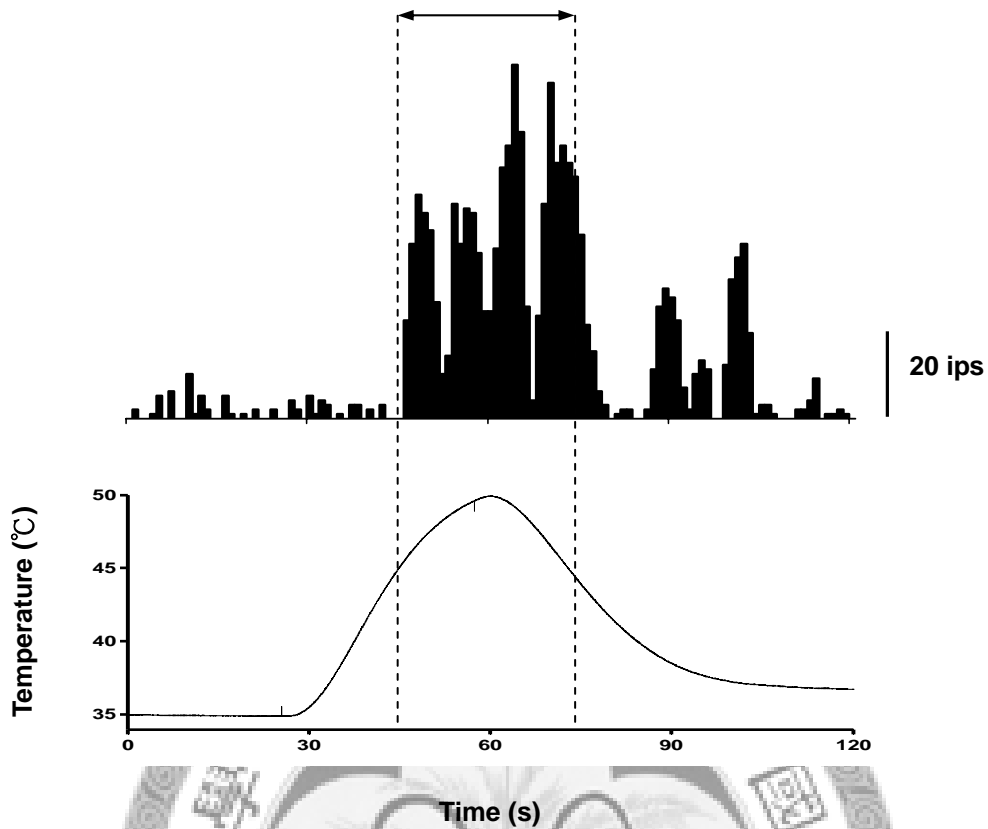


Figure 18: The analysis of the unit responses to contact thermal stimulation. Mean frequency of each unit was calculated in the 15s period before and after the peak temperature achieved, as shown within the bidirectional arrow in the rate histogram of the unit (upper panel). The changing curve of the stimulated temperature was shown in the lower panel.

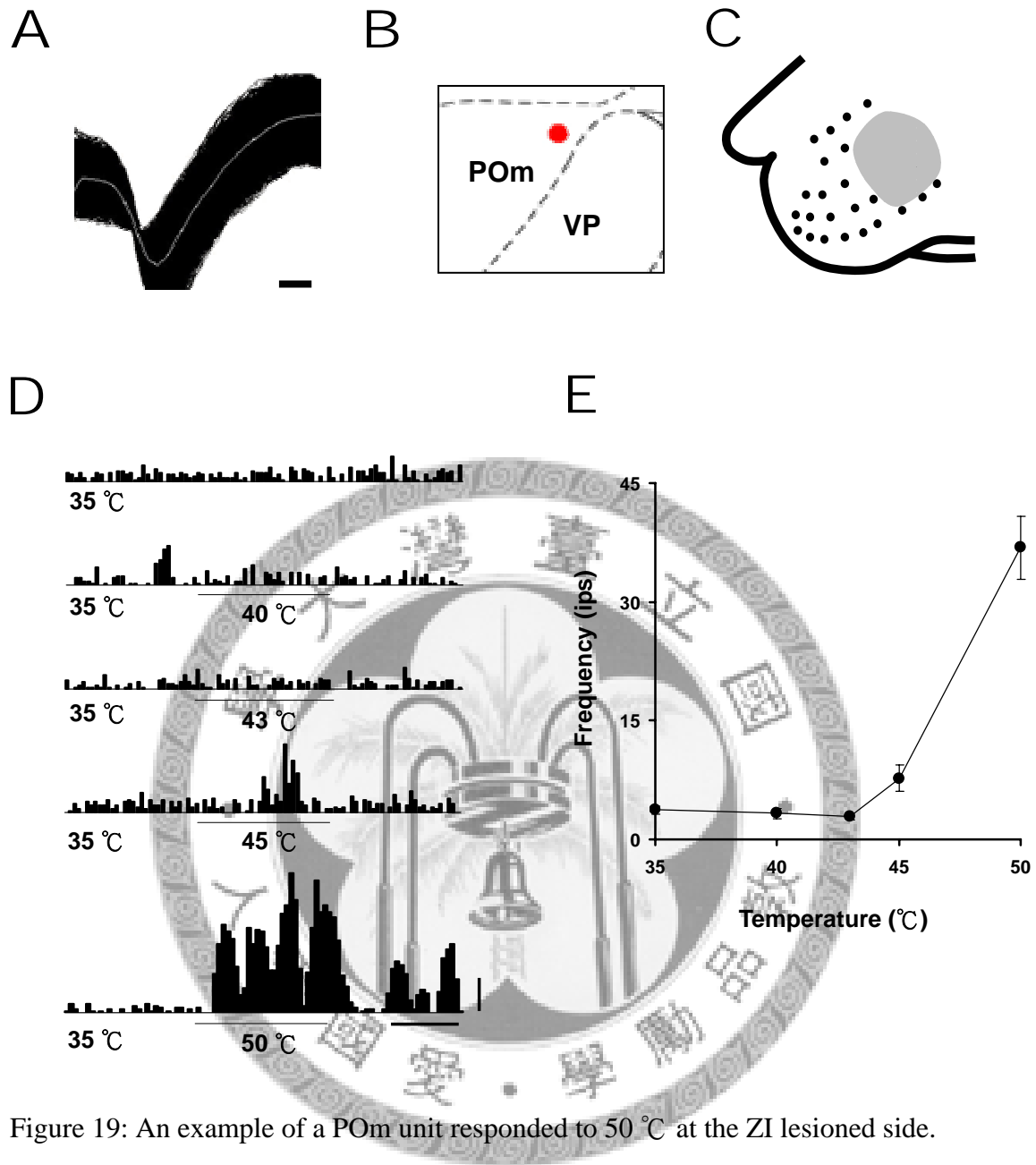


Figure 19: An example of a POM unit responded to 50 °C at the ZI lesioned side. Cumulative waveforms (A), unit location (B), and the receptive field (C) of the unit were shown. Responses of the unit were shown in histogram (D), and the stimulus-response curve was shown in (E). Scale bar in A: 100 μ s and in D: 20 ips, 15 s. Bin size: 1 s.

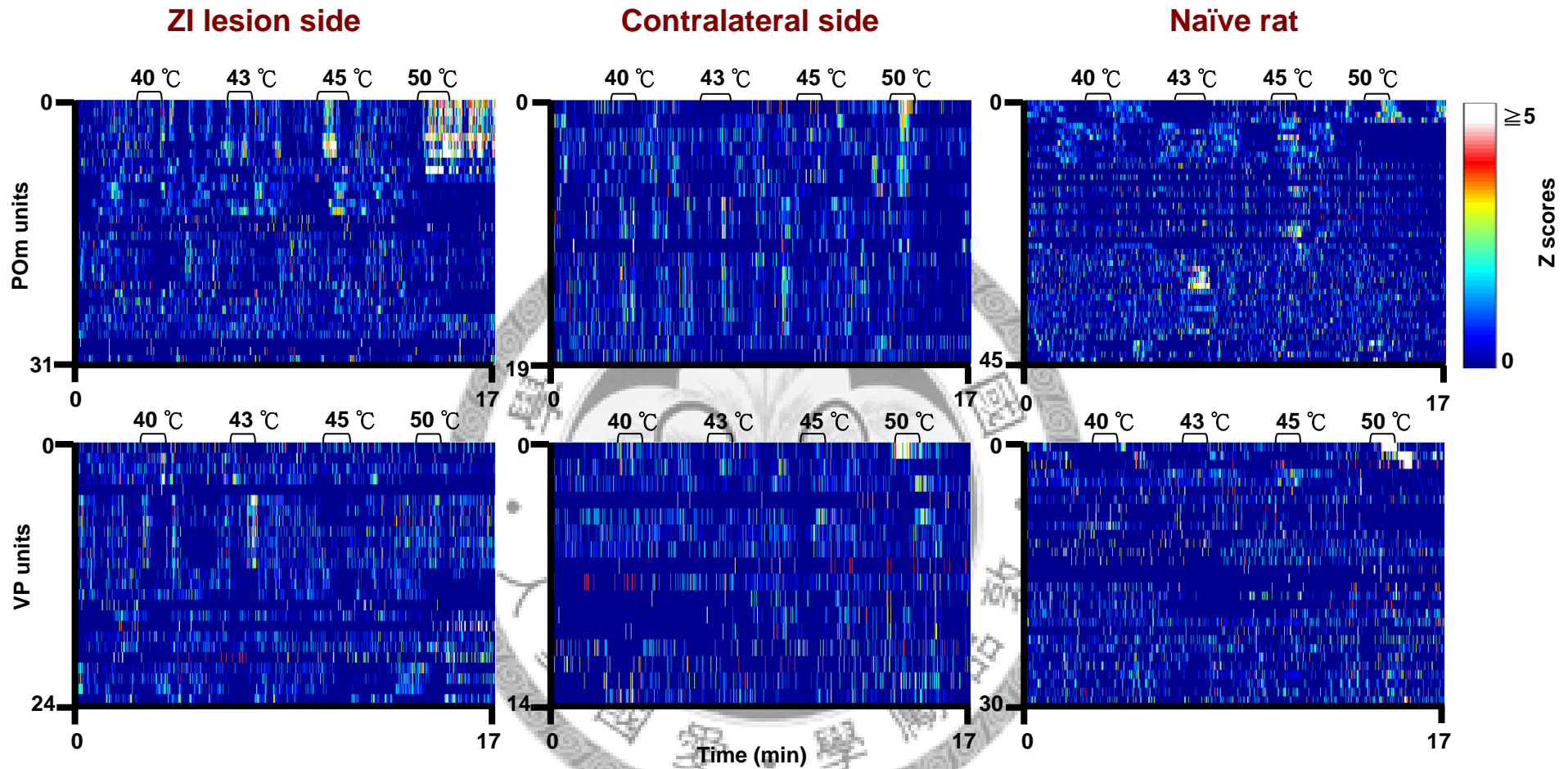


Figure 20: Ensemble responses of all units to the contact thermal stimulation. Upper plots from right to left were recorded in POm of ZI-lesion side, contralateral side, and naïve animal respectively. Lower plots from right to left were recorded in VP. Color scale represents the firing frequency in z-scores.

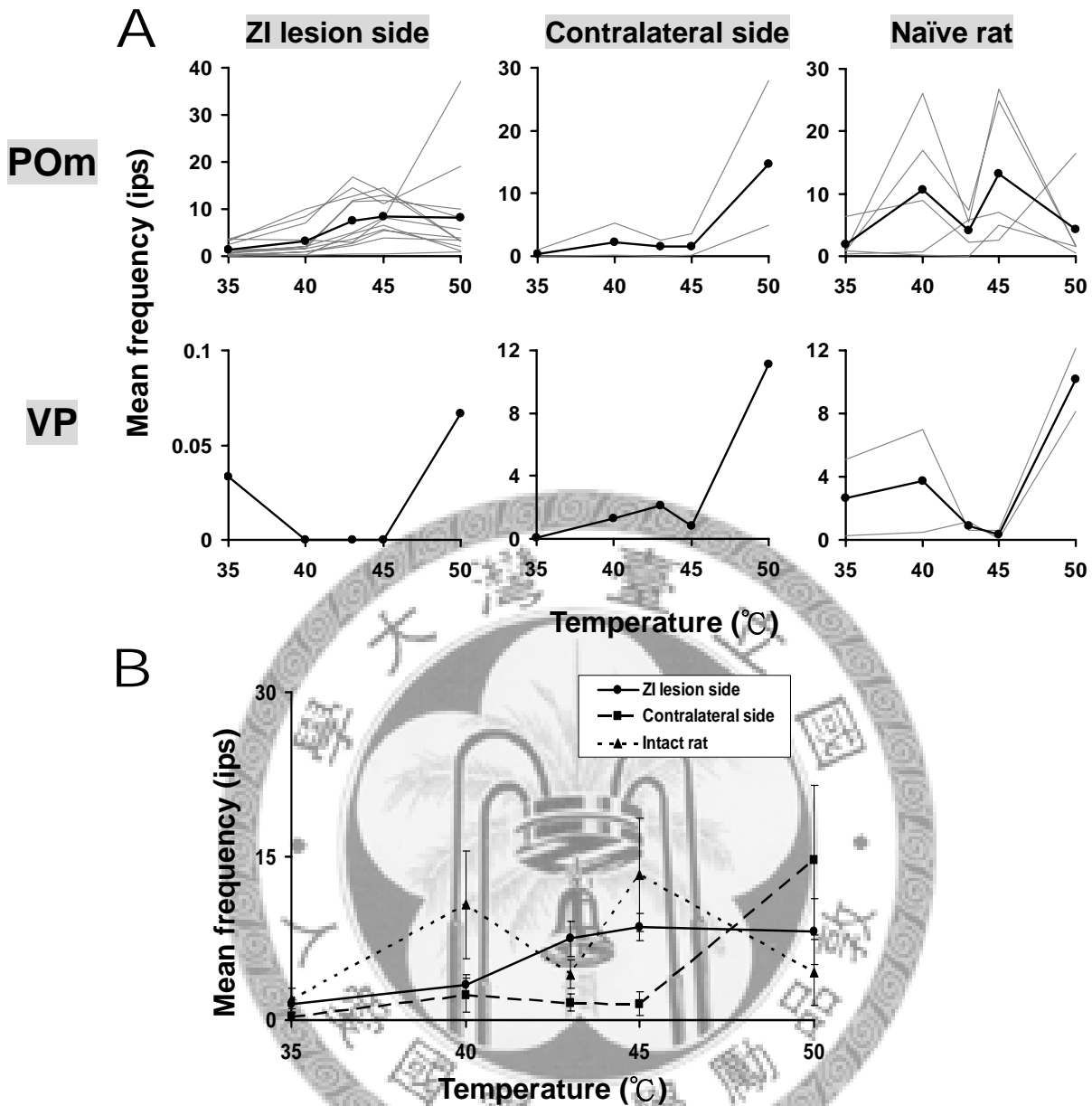
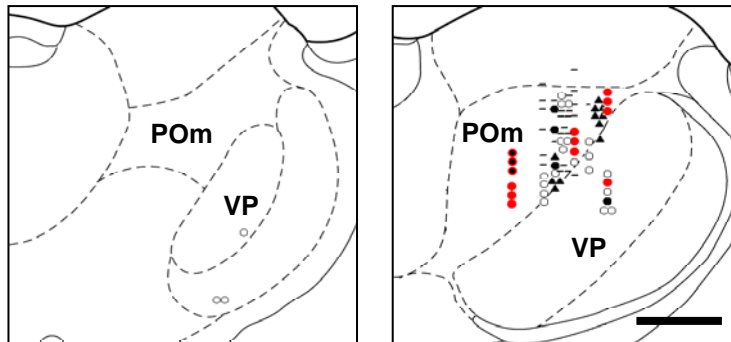
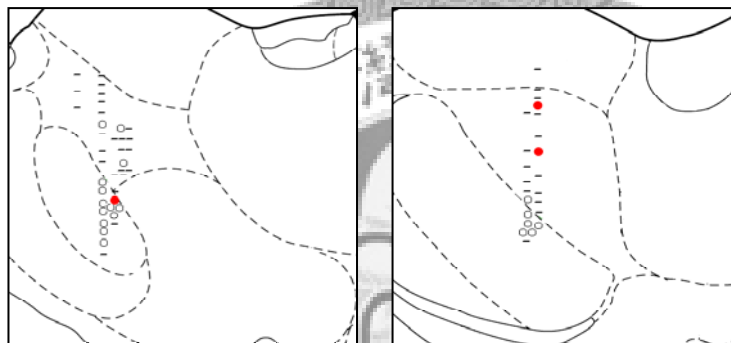


Figure 21: Stimulus- response curves of units responded to graded thermal stimuli. **A:** Stimulus- response curves of all P0m (upper panel) and VP (lower panel) units responded to noxious heat (45 °C or 50 °C) were shown as thin lines, and average response curves were shown as thick lines. From left to right are ZI lesion side, contralateral side, and intact animals, respectively. **B:** Average response curves of P0m units recorded in ZI lesion side (solid line), contralateral side (dashed line), and naïve animals (dotted line). The response pattern is no significant difference between groups. ($P > 0.05$; Two-way ANOVA, Tukey test) Error bars in **C** indicate standard errors of the mean.

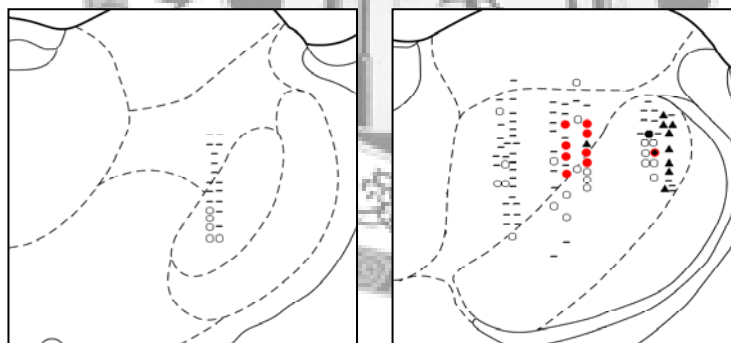
A ZI lesion side



B Contralateral side



C Naïve rat



P -2.6 mm

P -3.3 mm

- Tactile⁺ Pinch⁺
- ▲ Tactile⁻ Pinch⁺
- Tactile⁺ Pinch⁻
- Heat⁺
- No response

Figure 22: Locations of neurons recorded. **A to C**: Ipsilateral, contralateral to the ZI lesion side, and naïve animals. Red dots: units responsive only to noxious stimuli; Orange: units responsive to both noxious and innocuous stimuli; Green: units responsive only to innocuous stimuli; Gray: units show no responsiveness to mechanical stimulation. Scale bar: 0.5 cm. See figure 3 for abbreviations.